

Model-Free Nonlinear Feedback Optimization

Zhiyu He, Saverio Bolognani, Jianping He, Florian Dörfler, and Xinping Guan

Abstract—Feedback optimization is a control paradigm that enables physical systems to autonomously reach efficient operating points. Its central idea is to interconnect optimization iterations in closed-loop with the physical plant. Since iterative gradient-based methods are extensively used to achieve optimality, feedback optimization controllers typically require the knowledge of the steady-state sensitivity of the plant, which may not be easily accessible in some applications. In contrast, in this paper we develop a model-free feedback controller for efficient steady-state operation of general dynamical systems. The proposed design consists in updating control inputs via gradient estimates constructed from evaluations of the nonconvex objective at the current input and at the measured output. We study the dynamic interconnection of the proposed iterative controller with a stable nonlinear discrete-time plant. For this setup, we characterize the optimality and the stability of the closed-loop behavior as functions of the problem dimension, the number of iterations, and the rate of convergence of the physical plant. To handle general constraints that affect multiple inputs, we enhance the controller with Frank-Wolfe type updates.

Index Terms—Autonomous optimization, nonconvex optimization, gradient estimation.

I. INTRODUCTION

Efficient operation is a fundamental design goal for engineering systems, including (but not limited to) communication networks, power grids, transportation systems, and process control systems. Although numerical optimization methods [1] have been extensively studied as a way to obtain optimal decisions based on the exact abstraction of the problem, achieving the same on a real plant remains a challenging task. The main inhibiting factors include the absence of precise knowledge of plant models and the existence of unmeasured disturbances. For these reasons, the approach of first running an optimization program offline and then command its solution to a plant in a feedforward manner is rarely effective in practice. In contrast, feedback control based on real-time measurements is robust, albeit rarely optimal and able to handle constraints. Hence, many approaches have been developed to combine the complementary benefits of feedback control and feedforward optimization.

A. Related Work

Extremum seeking (ES) [2] is one of the first approaches that realized the above combination without relying on the plant model (*model-free*). It uses perturbations (e.g., sinusoidal signals) for exploration, collects measurements, estimates gradients via averaging, and then updates inputs.

Traditional ES is mostly suitable for low-dimensional systems, for which the orthogonality requirement on the elements of the perturbation signal is easy to satisfy [3]. To handle high dimensionality, stochastic ES with perturbations governed by stochastic processes [4] and Newton-based ES [5], [6] have been developed. However, the convergence is established in the asymptotic sense, without characterization of its dependence on the problem dimension and stability properties of the plant. Other work on stochastic ES adopts the perspective of stochastic approximation [7] and examines quadratic maps without dynamics [3]. Moreover, the common practice for ES to address constraints is to encode them in the objective via penalty functions [8]. This practice may not always guarantee precise constraint enforcement.

Reinforcement learning (RL) is another category of model-free approaches, through which agents interact with an uncertain environment, learn from the feedback, and make sequential decisions to maximize their cumulative reward [9]. This paper is, nonetheless, concerned with optimizing the steady-state operation of general stable dynamical systems, rather than the cumulative performance in the infinite horizon with the environment described by a Markov decision process [9].

As an emerging paradigm, feedback optimization (FO) [10], [11] offers a promising approach to drive general systems to efficient operating points, which constitute the optimal solutions of problems involving steady-state inputs and outputs. The key idea of FO is to implement optimization algorithms as feedback controllers, which are connected with physical plants to form a closed loop. Various approaches also share this closed-loop optimization viewpoint, including modifier adaptation [12], real-time iteration schemes [13], and real-time model predictive control [14]. Compared to these approaches, FO requires limited model information and less computational effort (see the review in [10]). By utilizing real-time measurements of system outputs, FO circumvents the need of accessing input-output models to evaluate the gradient of the objective function at the current operating point. Hence, the control inputs can be effectively updated also for problems with complex dynamics, e.g., real-time optimal power flow in electrical networks [15], [16] and congestion control in communication networks [17]. Furthermore, the feedback structure contributes to robustness against unmeasured disturbances and model mismatch [18], [19], as well as autonomous tracking of trajectories of optimal solutions of time-varying problems [20]–[25]. Some works [20], [22], [23], [26] consider fast-stable plants that are abstracted as algebraic steady-state maps. Others take system dynamics into account and characterize sufficient conditions for the closed-loop stability, including in continuous-time [21], [27]–[29] and sampled-data settings [30]. Specifically, among works that handle nonconvex objectives and nonlinear systems, [22], [26]

Z. He, J. He, and X. Guan are with the Department of Automation, Shanghai Jiao Tong University, and Key Laboratory of System Control and Information Processing, Ministry of Education of China, Shanghai 200240, China (emails: {hzy970920, jphe, xpguan}@sjtu.edu.cn). S. Bolognani and F. Dörfler are with the Automatic Control Laboratory, ETH Zürich, 8092 Zürich, Switzerland (emails: {bsaverio,dorfler}@ethz.ch).

address discrete-time systems represented by algebraic maps, while [28] tackles continuous-time systems. The results on nonconvex feedback optimization for discrete-time nonlinear dynamical systems are still lacking.

B. Motivations

FO requires limited model information, i.e., the sensitivity of the steady-state input-output map of the physical plant. Such information is needed because FO controllers update inputs via first-order methods (e.g., gradient [28], projected gradient [31] and primal-dual saddle-point methods [20], [21]). Given objective functions depending on steady-state inputs and outputs, due to the chain rule, their gradients with respect to inputs naturally contain the sensitivity terms. Recent works demonstrate that the sensitivity can be estimated based on system identification [19], recursive least-squares estimation [32], or data-driven methods that use past input-output data of open-loop linear systems [29], [33]. Nevertheless, on the one hand, the estimation can be a highly nontrivial task accompanied with errors, thus causing the approximate optimality of FO [18]. On the other hand, the uncertainties in and the complexity of engineering systems (e.g., volatile renewable energy sources in large-scale power systems [34]) may render the sensitivity of the plant costly to compute or even impossible to formulate, let alone feasible to estimate.

A different perspective offers us new insights to design an entirely model-free optimization-based feedback controller as in ES or RL. For current works on FO, it is the direct use of gradients in updates that leads to the requirement of the sensitivity. In other words, the key to model-free implementations lies in optimization without gradients. In fact, the key technique behind the elegant ES approach is an indirect way of learning gradients via perturbations and averaging, though restrictions exist when confronted with high-dimensional systems and constrained problems, and the core of policy gradient approaches to RL is expressing elusive performance gradients as simple expectations [35], [36]. In contrast, the so-called *zeroth-order optimization* [37] constructs gradient estimates [38]–[42] based on function evaluations and uses these estimates to form descent directions. Zeroth-order methods own comparable algorithmic structures and convergence rates with their first-order counterparts [37]. They are therefore well suited to serve as a building block for model-free FO.

C. Contributions

Motivated by the above observations, in this paper, we design a model-free feedback controller for efficient steady-state operation of discrete-time nonlinear dynamical systems, where the efficiency is quantified by nonconvex objective functions of inputs and outputs. To gain robustness against unmeasured disturbances, we inherit from ES and FO the idea of using the measurements of outputs and implementing optimization-based controllers in closed loop. More importantly, to facilitate complete model-free operation, we update control inputs based on gradient estimates constructed from current and previous evaluations of objective functions. Our analysis takes a stochastic perspective, and we explicitly characterize

TABLE I
COMPARISON OF WORKS ON FO WITH THE UNKNOWN SENSITIVITY

Works	[29], [33]	[32]	[23]	this work
Nonconvex Objectives				✓
Input Constraints	✓	✓	✓	✓
Plant Model	linear dynamic	linear algebraic	linear algebraic	nonlinear dynamic
Method	data-driven sensitivity estimation based on input-output trajectories	recursive least-squares sensitivity estimation	two-point symmetric gradient estimation	residual one-point gradient estimation

the optimality (measured by the expected squared norm of gradients, which gives the first-order stationary condition) in terms of the problem dimension and the stability properties of the plant. The analysis relies on the establishment of recursive inequalities of both the expected values of the Lyapunov function of the system and the second moments of gradient estimates along descent steps of the controller. Then, with the interconnection of the plant and the controller, the coupled decay of the above two quantities are synthesized to obtain a bound on the convergence measure. This path of analysis is different from those took by the related literature, e.g., singular perturbation analysis [10], [27], [28], LMI stability certificates [21], and invariance principles [26]. We also elaborate on the extension to tackle coupling constraints on the inputs via Frank-Wolfe type updates. In Table I, we compare various works on FO addressing the unknown sensitivity of the plant.

The main contributions are summarized as follows.

- To the best of our knowledge, this is the first work on feedback optimization while considering nonconvex objectives and nonlinear discrete-time dynamical systems in both the unconstrained and constrained settings.
- We propose a novel model-free feedback controller that drives the system to the solution of a given optimization problem by updating control inputs via gradient estimates. These estimates are obtained from present and past evaluations of the objective at inputs and measured outputs and do not depend on any prior model information.
- We explicitly characterize the optimality of closed-loop solutions. It is measured by the second moment of the gradient of the objective function in the unconstrained scenario, and by the expected Frank-Wolfe dual gap in the setting with input constraint sets. We demonstrate that the optimality scales polynomially with the problem dimension and the reciprocal of the number of iterations, and we quantify its dependence on the stability properties of the physical plant.

D. Organization

The rest of this paper is organized as follows. Section II formally defines the problem of interests and provides some preliminaries. In Section III, we present the proposed model-free nonconvex feedback optimization controller. Section IV

provides the performance analysis of the interconnection of the controller and the dynamical plant. The extension to handle input constraint sets is explored in Section V, followed by numerical evaluations in Section VI. Finally, in Section VII, we conclude the paper and discuss some future directions.

II. PROBLEM FORMULATION AND PRELIMINARIES

A. Problem Formulation

Consider the discrete-time dynamical system

$$\begin{aligned} x_{k+1} &= f(x_k, u_k, d), \\ y_k &= g(x_k, d), \end{aligned} \quad (1)$$

where at time k , $x_k \in \mathbb{R}^n$ is the system state, $u_k \in \mathbb{R}^p$ is the control input, $y_k \in \mathbb{R}^q$ is the measured output, and $d \in \mathbb{R}^r$ is the unknown constant exogenous disturbance.

Assumption 1. *The system (1) is globally exponentially stable with constant inputs, i.e., with $u_k = u, \forall k \in \mathbb{N}$. Moreover, there exists a unique steady-state map $x_{ss} : \mathbb{R}^p \times \mathbb{R}^r \rightarrow \mathbb{R}^n$ such that $\forall u, d, f(x_{ss}(u, d), u, d) = x_{ss}(u, d)$. The map $x_{ss}(u, d)$ is M_x -Lipschitz with respect to u , and the function $g(x, d)$ is M_g -Lipschitz with respect to x .*

The above properties of the map $x_{ss}(u, d)$ can be ensured by, e.g., the implicit function theorem [43, 1B.1]. For instance, x_{ss} is well defined and Lipschitz continuous in a neighborhood of (u, d) when $f(x, u, d) - x$ is continuously differentiable with respect to x and $\nabla_x f(x, u) - I$ is nonsingular. Based on Assumption 1, in a steady state we have

$$y = g(x_{ss}(u, d), d) \triangleq h(u, d). \quad (2)$$

Additionally, the standard converse Lyapunov theorem [44], [45] guarantees that there exist a Lyapunov function $V : \mathbb{R}^n \times \mathbb{R}^p \times \mathbb{R}^r \rightarrow \mathbb{R}$ and parameters $\alpha_1, \alpha_2, \alpha_3 > 0$ such that

$$\alpha_1 \|x - x_{ss}(u, d)\|^2 \leq V(x, u, d) \leq \alpha_2 \|x - x_{ss}(u, d)\|^2, \quad (3)$$

$$V(f(x, u, d), u, d) - V(x, u, d) \leq -\alpha_3 \|x - x_{ss}(u, d)\|^2. \quad (4)$$

Based on (3) and (4), we can define the rate of change of the function value $V(x_k, u_k, d)$ as

$$\mu \triangleq \frac{2\alpha_2}{\alpha_1} \left(1 - \frac{\alpha_3}{\alpha_2}\right). \quad (5)$$

Assumption 2. *The rate of change μ satisfies $\mu < 1$.*

A smaller μ implies a faster rate at which the system reaches its steady state. It is typically small in sampled-data settings with large sampling periods [30]. A formal interpretation of this constant will be presented later in Lemma 3.

We then consider the optimization problem

$$\begin{aligned} \min_{u, y} \quad & \Phi(u, y) \\ \text{s.t.} \quad & y = h(u, d), \end{aligned} \quad (6)$$

where $\Phi(u, y)$ is the objective function, and $y = h(u, d)$ is the steady-state map (2). By eliminating the variable y , we transform problem (6) to an unconstrained optimization problem in the control input, i.e.,

$$\min_u \quad \tilde{\Phi}(u), \quad (7)$$

where $\tilde{\Phi}(u) \triangleq \Phi(u, h(u, d))$.

Assumption 3. *The function $\tilde{\Phi}(u)$ is M -Lipschitz, and $\inf_{u \in \mathbb{R}^p} \tilde{\Phi}(u) > -\infty$. The function $\Phi(u, y)$ is M_y -Lipschitz with respect to y .*

The requirements on Lipschitz continuity in Assumption 3 are common and largely satisfied in applications.

Standard numerical optimization [1] requires the exact knowledge of the map h and the disturbance d to solve (6) or, equivalently, (7). As discussed in Section I, this approach may be impractical in many applications. In contrast, in this paper, we aim to design a model-free feedback controller that utilizes real-time measurements of y to drive the system (1) to efficient steady-state operating conditions, as defined by problem (6). The challenges come from the nonconvexity of the objective function, the dynamics of the nonlinear plant, and the goal of being fully model-free.

B. Preliminaries of Zeroth-Order Optimization

The key idea of zeroth-order optimization is to utilize function evaluations to construct gradient estimates, thus eliminating the need of accessing gradients directly. The design of this work is inspired by the gradient estimate based on residual feedback in [42], which owns comparable performance with the mainstream two-point gradient estimates [38]–[40]. However, it is significantly easier to implement in the context of FO, as we will see below.

For an objective function $\xi(w) : \mathbb{R}^p \rightarrow \mathbb{R}$, the gradient estimate proposed in [42] is

$$\widehat{\nabla} \xi(w_k) = \frac{v_k}{\delta} (\xi(w_k + \delta v_k) - \xi(w_{k-1} + \delta v_{k-1})), \quad (8)$$

where v_k and v_{k-1} are independent random vectors drawn from the standard multivariate normal distribution, and $\delta > 0$ is a smoothing parameter. Note that the objective value evaluated at the previous time $k-1$ is reused in the current iteration k . Hence, for (8), only a single new evaluation of ξ is required in each iteration. In contrast, a standard two-point gradient estimate requires two function evaluations, which would translate to two actuation steps in an FO setting; see also Remark 1 below.

According to [42, Lemma 3.1], $\widehat{\nabla} \xi(w_k)$ in (8) is an unbiased estimate of the gradient of the Gaussian smooth approximation $\xi_\delta(w)$ for $\xi(w)$ at w_k , where

$$\xi_\delta(w) = \mathbb{E}_{v \sim \mathcal{N}(0, I)} [\xi(w + \delta v)]. \quad (9)$$

We summarize the properties of $\xi_\delta(w)$ as follows.

Lemma 1 ([38]). *If $\xi : \mathbb{R}^p \rightarrow \mathbb{R}$ is M_ξ -Lipschitz, then for any $w \in \mathbb{R}^p$, $\delta > 0$, and $\xi_\delta(w)$ given by (9),*

$$|\xi_\delta(w) - \xi(w)| \leq \delta M_\xi \sqrt{p},$$

and $\xi_\delta(w)$ is $\frac{M_\xi \sqrt{p}}{\delta}$ -smooth, i.e., its gradients are $\frac{M_\xi \sqrt{p}}{\delta}$ -Lipschitz continuous.

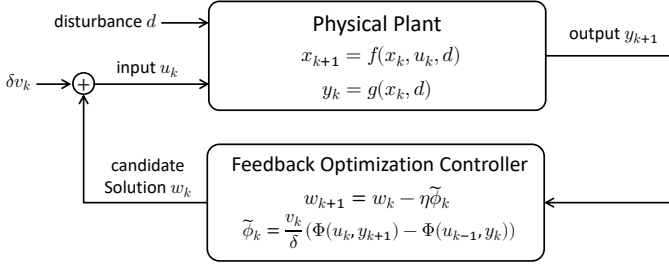


Fig. 1. An illustration of the interconnection of the physical plant and the model-free feedback optimization controller.

III. DESIGN OF MODEL-FREE FEEDBACK OPTIMIZATION

The proposed controller iteratively updates control inputs along descent steps for the objective function $\tilde{\Phi}(u)$. These steps are given by the negative gradient estimates constructed from the evaluations of $\tilde{\Phi}(u)$. Such a design does not involve the sensitivity $\nabla_u h(u, d)$ of the steady-state input-output map $h(u, d)$ and therefore makes this controller inherently model-free. An illustration of the interconnection of the system (1) and this controller is provided in Fig. 1.

The proposed feedback optimization controller is

$$w_{k+1} = w_k - \eta \tilde{\phi}_k, \quad (10a)$$

$$\tilde{\phi}_k = \frac{v_k}{\delta} (\Phi(u_k, y_{k+1}) - \Phi(u_{k-1}, y_k)), \quad (10b)$$

$$u_{k+1} = w_{k+1} + \delta v_{k+1}, \quad (10c)$$

where v_k, v_{k-1} are standard normal random vectors, and δ is a smoothing parameter as in (8). The update (10) describes the actions performed by the controller at time $k+1$. First, a new candidate solution w_{k+1} is computed based on $\tilde{\phi}_k$, which is the gradient estimate at the previous candidate solution w_k . This estimate is constructed once the measurement y_{k+1} is available, since y_{k+1} reflects the influence of u_k and is utilized as a substitute for the steady-state output $h(u_k, d)$. Notice that the historic evaluation $\Phi(u_{k-1}, y_k)$ is reused at time $k+1$. Finally, the new input u_{k+1} is obtained by perturbing the candidate solution w_{k+1} with the exploration noise δv_{k+1} , and it is applied to the system (1). The role of the perturbation δv_k is to explore (1) around w_k , thus contributing to the effectiveness of $\tilde{\phi}_k$ as a gradient estimate.

Remark 1. The gradient estimate (10b) is inspired by the estimate based on residual feedback in [42]. Nonetheless, there exists a key difference in that it uses the approximate objective value $\Phi(u_k, y_{k+1})$ based on real-time measurements of system outputs, rather than the exact objective value $\tilde{\Phi}(u_k) = \Phi(u_k, h(u_k, d))$. This feature results from the consideration of system dynamics, which prevents us from instantly accessing steady-state outputs. The errors incurred by the approximations pose additional challenges for the closed-loop performance analysis and will be one of the main foci of the following section.

IV. PERFORMANCE ANALYSIS

In this section, we analyze the performance of implementing the proposed feedback optimization controller (10) in closed loop with the system (1). We first establish some supporting

lemmas on the bounds and recursive inequalities of certain important variables. Then, we present our performance certificate and discuss its implications.

A. Supporting Lemmas

First, we provide an upper bound for the error in the evaluation of $\Phi(u, h(u, d))$. Such an error results from the substitution of the measurement y_{k+1} for the steady-state output $h(u_k, d)$ and is defined as

$$e_\Phi(x_k, u_k) \triangleq \Phi(u_k, y_{k+1}) - \Phi(u_k, h(u_k, d)).$$

Lemma 2. If Assumptions 1 and 3 hold, then

$$|e_\Phi(x_k, u_k)|^2 \leq \frac{\mu M_y^2 M_g^2}{2\alpha_2} V(x_k, u_k, d). \quad (11)$$

Proof. Please see Appendix A. \square

The right-hand side of (11) involves the Lyapunov function V and the parameters $\alpha_1, \alpha_2, \alpha_3$ corresponding to (1). It reflects the rate at which the system reaches the steady state, and quantifies the closeness between $\Phi(u_k, y_{k+1})$ and $\tilde{\Phi}(u_k)$.

In the following lemmas, we establish the recursive inequalities of two key quantities. One is the expected value of the Lyapunov function $V(x_k, u_k, d)$, i.e., $\mathbb{E}_{v_{[k]}}[V(x_k, u_k, d)]$, which measures how close the current state x_k is to the steady state $x_{ss}(u_k, d)$. The other is the second moment of the gradient estimate $\tilde{\phi}_k$, i.e., $\mathbb{E}_{v_{[k]}}[\|\tilde{\phi}_k\|^2]$, which reflects the stationary condition at the solution w_k . Note that $v_{[k]} \triangleq (v_0, \dots, v_k)$, and that $\mathbb{E}_{v_{[k]}}$ denotes the expectation with respect to $v_{[k]}$. Also recall that u_k and v_k are p -dimensional vectors.

Lemma 3. If Assumptions 1 and 3 hold, with (10), we have

$$\begin{aligned} & \mathbb{E}_{v_{[k]}}[V(x_k, u_k, d)] \\ & \leq \mu \mathbb{E}_{v_{[k]}}[V(x_{k-1}, u_{k-1}, d)] \\ & \quad + 4\alpha_2 \eta^2 M_x^2 \mathbb{E}_{v_{[k]}}[\|\tilde{\phi}_{k-1}\|^2] + 8\alpha_2 p \delta^2 M_x^2. \end{aligned} \quad (12)$$

Proof. Please see Appendix B. \square

Lemma 4. If Assumptions 1 and 3 hold, with (10), we have

$$\begin{aligned} & \mathbb{E}_{v_{[k]}}[\|\tilde{\phi}_k\|^2] \\ & \leq \frac{6}{\delta^2} M^2 \eta^2 p \mathbb{E}_{v_{[k]}}[\|\tilde{\phi}_{k-1}\|^2] + 24M^2(p+4)^2 \\ & \quad + \frac{3\mu M_y^2 M_g^2}{2\alpha_2 \delta^2} ((p+4) \mathbb{E}_{v_{[k]}}[V(x_k, u_k, d)] \\ & \quad + p \mathbb{E}_{v_{[k]}}[V(x_{k-1}, u_{k-1}, d)]). \end{aligned} \quad (13)$$

Proof. Please see Appendix C. \square

From (12) and (13), we observe that the decay of the sequences $\{\mathbb{E}_{v_{[k]}}[V(x_k, u_k, d)]\}$ and $\{\mathbb{E}_{v_{[k]}}[\|\tilde{\phi}_k\|^2]\}$ are coupled with each other. Based on the above lemmas, we can obtain the upper bounds on the partial sums of these two sequences and then use these bounds to quantify the optimality in the following performance analysis.

B. Performance Certificate

We characterize the performance of the interconnection of the controller (10) and the system (1). Recall that $\tilde{\Phi}_\delta$ is the Gaussian smooth approximation for $\tilde{\Phi}$ (see (9)), where δ is a smoothing parameter. Let $\epsilon > 0$ be a given desired precision of this approximation, and let us choose $\delta = \frac{\epsilon}{M\sqrt{p}}$ so that Lemma 1 ensures that $|\tilde{\Phi}_\delta(u) - \tilde{\Phi}(u)| \leq \epsilon^1$. Additionally, let $T \in \mathbb{N}_+$ be a number of iterations set beforehand, and recall that p is the size of the input. The following theorem shows how to choose the constant step size η based on ϵ , T and p , and what performance guarantee follows from these choices.

Theorem 5. *Suppose that Assumptions 1-3 hold. For a precision $\epsilon > 0$, let $\delta = \frac{\epsilon}{M\sqrt{p}}$, and let $0 < \eta < \frac{\kappa^* \sqrt{\epsilon}}{p^{\frac{3}{2}} \sqrt{T}}$, where*

$$\kappa^* = \mathcal{O}\left(\min\left\{\frac{1-\mu}{\sqrt{\mu}}, 1-\sqrt{\mu}\right\} \cdot \sqrt{pT\epsilon}\right)$$

is the upper bound determined by (50) in Appendix F. The closed-loop interconnection of (1) and (10) ensures that

$$\begin{aligned} & \frac{1}{T} \sum_{k=0}^{T-1} \mathbb{E}_{v_{[T-1]}} [\|\nabla \tilde{\Phi}_\delta(w_k)\|^2] = \\ & \mathcal{O}\left(\frac{p^{\frac{3}{2}}}{\sqrt{\epsilon T}(1-\rho)}\right) + \mathcal{O}\left(\frac{p^2 \sqrt{\mu}}{1-\rho} \cdot \left(1 + \frac{1}{T\epsilon^2 \alpha_2}\right)\right), \end{aligned} \quad (14)$$

where $\rho \in (0, 1)$ is the spectral radius of the matrix C' given by (46) in Appendix F. Moreover,

$$\rho = \mathcal{O}\left(\max\left(\frac{1}{Tp\epsilon}, \mu\right) + \left(\frac{\mu}{Tp\epsilon}\right)^{\frac{1}{2}}\right).$$

Proof. Please see Appendix F. \square

In Theorem 5, we use the average second moments of the gradients of the Gaussian smooth approximation $\tilde{\Phi}_\delta(u)$ as the convergence measure. This measure is common in the field of zeroth-order nonconvex optimization [38], [42], [46], where nonconvexity inhibits the investigation of optimality gaps, and stochasticity required by exploration noises in gradient estimates leads to the consideration of *ergodic* rates.

In the right-hand side of (14), the first term reflects the order of optimality concerning the descent-based update of the proposed controller, whereas the second term corresponds to the order of errors resulting from the relatively slow response of the system excited by the controller (10). If the system is rapidly decaying, i.e., μ is very close to 0, then the aforementioned second term can be neglected, and

$$\frac{1}{T} \sum_{k=0}^{T-1} \mathbb{E}_{v_{[T-1]}} [\|\nabla \tilde{\Phi}_\delta(w_k)\|^2] = \mathcal{O}\left(\frac{p^{\frac{3}{2}}}{\sqrt{\epsilon T}(1-\rho)}\right), \quad (15)$$

where the order of ρ is $\mathcal{O}(1/Tp\epsilon)$ in this case. Note that the right-hand side of (15) approaches 0 as $T \rightarrow \infty$.

Moreover, in the transient stage of iterations (i.e. at time $k = 0, \dots, T-1$), w_k comprises the set of candidate solutions, while u_k is the actual input obtained by perturbing w_k (see

¹Ideally, any $\delta \in (0, \frac{\epsilon}{M\sqrt{p}}]$ would yield the desired precision. In practice, however, the largest possible δ makes the gradient estimate (10b) more robust to possible measurement noise [37].

(10c)) and fed into the system. Theorem 5 characterizes optimality in terms of w_k . In the following corollary, we quantify sub-optimality in terms of u_k aligned with the objective (7).

Corollary 1. *If the conditions of Theorem 5 hold, then*

$$\begin{aligned} & \frac{1}{T} \sum_{k=0}^{T-1} \mathbb{E}_{v_{[T-1]}} [\|\nabla \tilde{\Phi}_\delta(u_k)\|^2] \\ & \leq \frac{2}{T} \sum_{k=0}^{T-1} \mathbb{E}_{v_{[T-1]}} [\|\nabla \tilde{\Phi}_\delta(w_k)\|^2] + 2M^2 p^2. \end{aligned} \quad (16)$$

Proof. Please see Appendix G. \square

Finally, we characterize the closed-loop stability properties.

Theorem 6. *If the conditions of Theorem 5 hold, then,*

$$\begin{aligned} & \frac{1}{T} \sum_{k=0}^{T-1} \mathbb{E}_{v_{[T-1]}} [\|x_{k+1} - x_{ss}(u_k, d)\|^2] \\ & = \mathcal{O}\left(\frac{\epsilon^{\frac{3}{2}} \sqrt{\mu}}{\sqrt{pT}(1-\rho)}\right) + \mathcal{O}\left(\frac{(\epsilon^2 + \frac{1}{T\alpha_2})\mu}{1-\rho}\right). \end{aligned} \quad (17)$$

Proof. Please see Appendix H. \square

In Theorem 6, we focus on the average second moments of the distances between the state x_{k+1} after u_k is applied at time k and the steady state $x_{ss}(u_k, d)$. Theorem 6 suggests that the closed-loop stability properties heavily depend on the rate of change μ defined in (5). In fact, for a rapidly decaying system (i.e., with a μ very close to 0), the right-hand side of (17) is also approximately 0.

V. EXTENSION TO CONSTRAINED INPUT

We now present the extension of the proposed model-free feedback optimization controller to handle input constraints.

A common type of such constraints is represented by input saturation that results from actuation limits or actions of low-level controllers [10]. To tackle these constraints, we can directly implement the proposed controller (10) and outsource the constraint enforcement to the physical plant. For instance, consider the following system with the saturated control input

$$\begin{aligned} x_{k+1} &= f(x_k, \text{sat}(u_k), d) \triangleq \tilde{f}(x_k, u_k, d), \\ y_k &= g(x_k, d), \end{aligned} \quad (18)$$

where $\text{sat}(u_k)$ equals to u_k if u_k falls in the constraint set \mathcal{U} , and it equals to some limit value otherwise. Since $\text{sat}(\cdot)$ will not change the Lipschitz continuity of the corresponding steady-state map and the objective function, the controller (10) can still drive the system (18) to its efficient operating point, while the constraint \mathcal{U} is naturally enforced by the physical plant through saturation effects.

In the remainder of this section, we focus on coping with other general engineering constraints that may couple multiple inputs, are not enforced by low-level saturation, and therefore need to be accounted for in the controller design.

A. Problem Reformulation and Preliminaries

Let the input constraint set be denoted by $\mathcal{U} \subset \mathbb{R}^p$. In this case, the optimization problem becomes

$$\begin{aligned} \min_{u,y} \quad & \Phi(u, y) \\ \text{s.t.} \quad & y = h(u, d), \\ & u \in \mathcal{U}. \end{aligned} \quad (19)$$

Problem (19) can be equivalently reformulated as

$$\min_u \quad \tilde{\Phi}(u), \quad \text{s.t. } u \in \mathcal{U}, \quad (20)$$

where $\tilde{\Phi}(u) \triangleq \Phi(u, h(u, d))$. We accordingly modify the requirement on the finite infimum in Assumption 3 to

$$\inf_{u \in \mathcal{U}} \tilde{\Phi}(u) > -\infty. \quad (21)$$

The assumption on \mathcal{U} is given as follows.

Assumption 4. *The set \mathcal{U} is convex, closed, and bounded with diameter D .*

In applications, there are usually upper and lower bounds that define the admissible input [10], which translates to the bounded constraint set. It follows from Assumption 4 that $\forall u_1, u_2 \in \mathcal{U}, \|u_1 - u_2\| \leq D$. Notice that D is not involved in the updates of the controller and is only used in the performance analysis. The existence of \mathcal{U} renders the standard normal random vectors v_k utilized in the previous sections unfavorable, since the unboundedness of Gaussian distributions may cause the perturbed input $u_k = w_k + \delta v_k$ to lie far outside \mathcal{U} . Instead, we uniformly sample v_k from the unit sphere $\mathbb{S}_{p-1} \triangleq \{v \in \mathbb{R}^p : \|v\| = 1\}$. This scheme of sampling is also adopted by [40], [47], [48]. In this case, the smooth approximation $\tilde{\Phi}_\delta(w)$ for the objective $\tilde{\Phi}(w)$ is

$$\tilde{\Phi}_\delta(w) = \mathbb{E}_{v \sim U(\mathbb{B}_p)}[\tilde{\Phi}(w + \delta v)], \quad (22)$$

where $U(\mathbb{B}_p)$ is the uniform distribution over the closed unit ball \mathbb{B}_p in \mathbb{R}^p . Similar to Lemma 1, the properties of $\tilde{\Phi}_\delta(w)$ are summarized as follows.

Lemma 7. *If $\tilde{\Phi} : \mathbb{R}^p \rightarrow \mathbb{R}$ is M -Lipschitz, then for any $w \in \mathbb{R}^p$, $\delta > 0$, and $\tilde{\Phi}_\delta(w)$ defined in (22),*

$$\mathbb{E}_{v \in U(\mathbb{S}_{p-1})} \left[\frac{p}{\delta} \tilde{\Phi}(w + \delta v) \right] = \nabla \tilde{\Phi}_\delta(w), \quad (23a)$$

$$|\tilde{\Phi}_\delta(w) - \tilde{\Phi}(w)| \leq M\delta, \quad (23b)$$

and $\tilde{\Phi}_\delta(w)$ is $\frac{Mp}{\delta}$ -smooth, i.e., its gradients are $\frac{Mp}{\delta}$ -Lipschitz continuous.

Proof. The equation (23a) is proved in [41, Lemma 2.1]. The proofs of (23b) and the smoothness of $\tilde{\Phi}_\delta(w)$ are similar to those of [47, Lemma 4.1], where $\tilde{\Phi}(w)$ is assumed to be a smooth function. \square

B. Design of Constrained Feedback Optimization

In the input-constrained case, the updates of the proposed model-free feedback optimization controller are

$$w_{k+1} = (1 - \eta)w_k + \eta s_k, \quad (24a)$$

$$s_k = \arg \min_{s \in \mathcal{U}} \langle s, \tilde{\phi}_k \rangle, \quad (24b)$$

$$\tilde{\phi}_k = \frac{pv_k}{\delta} (\Phi(u_k, y_{k+1}) - \Phi(u_{k-1}, y_k)), \quad (24c)$$

$$u_{k+1} = w_{k+1} + \delta v_{k+1}, \quad (24d)$$

where $v_k, v_{k+1} \sim U(\mathbb{S}_{p-1})$ are uniformly sampled from the unit sphere \mathbb{S}_{p-1} , δ is a smoothing parameter, and $\eta \in (0, 1)$. The initial point w_0 is chosen from the constraint set \mathcal{U} . The update (24) is based on the Frank-Wolfe algorithm for constrained optimization [49], combined with the residual one-point gradient estimation that we have already seen before in (10). At time $k + 1$, the controller calculates a new candidate solution w_{k+1} by taking a convex combination of the previous solution w_k and a new point s_k . Note that s_k is obtained in the step of linear minimization constrained over \mathcal{U} , where the gradient estimate $\tilde{\phi}_k$ corresponding to w_k is utilized. Similar to (10), $\tilde{\phi}_k$ is constructed when the output measurement y_{k+1} is at hand. Finally, the controller applies the input u_{k+1} perturbed with the exploration noise δv_{k+1} to the system (1).

Remark 2. *Compared to zeroth-order Frank-Wolfe algorithms [48], [50], [51] that use two-point estimates, in (24c), we use the current and the historic evaluations of the objective function to construct the gradient estimate. This design corresponds to the scenario where for a dynamic plant, at every time $k + 1$, we can only obtain one new approximate objective value $\Phi(u_k, y_{k+1})$ based on the real-time measurement y_{k+1} .*

C. Performance Analysis

We use the Frank-Wolfe gap, i.e.,

$$\mathcal{G}(w_k) = \max_{w \in \mathcal{U}} \langle w - w_k, -\nabla \tilde{\Phi}_\delta(w_k) \rangle \quad (25)$$

to measure optimality at w_k . In (25), $\tilde{\Phi}_\delta$ is the smooth approximation for $\tilde{\Phi}$ (see (22)), and δ is a smoothing parameter. Note that $\mathcal{G}(w_k)$ is non-negative for any $w_k \in \mathcal{U}$, and equals 0 if and only if w_k is a stationary point of $\tilde{\Phi}_\delta(w)$ [48].

As before, let ϵ be the user-specified precision of the smooth approximation, and let us choose $\delta = \frac{\epsilon}{M}$ so that Lemma 7 ensures that $|\tilde{\Phi}_\delta(u) - \tilde{\Phi}(u)| \leq \epsilon$. Similarly to Theorem 5, the following theorem demonstrates how to choose the constant step size η based on ϵ , the pre-set number of iterations T , and the input size p , and what performance guarantee follows from these choices.

Theorem 8. *Suppose that Assumptions 1-4 hold. Let $\delta = \frac{\epsilon}{M}$, $\eta = \kappa \sqrt{\frac{\epsilon}{pT}}$, where $\kappa \in (0, \frac{\sqrt{pT}}{\sqrt{\epsilon}})$. For the closed-loop interconnection of (1) and (24), we have*

$$\begin{aligned} & \frac{1}{T} \sum_{k=1}^T \mathbb{E}_{v_{[T]}} [\mathcal{G}(w_k)] \leq \\ & \left(\frac{\mathbb{E}_{v_{[T]}} [\tilde{\Phi}_\delta(w_1)] - \tilde{\Phi}_\delta^*}{\kappa} + \frac{D^2 M^2 \kappa}{2} \right) \sqrt{\frac{p}{\epsilon T}} + D \left\{ \right. \\ & 6M^4 D^2 \kappa^2 \cdot \frac{p}{\epsilon T} + 24M^2 p^2 + \frac{\mu M_y^2 M_g^2}{2\alpha_2} \\ & \cdot \left. \left[\frac{1 + \mu}{(1 - \mu)T} \cdot \left(E_{v_{[T]}} [V(x_0, u_0, d)] \right) \right] \right\} \end{aligned}$$

$$\begin{aligned}
& + 2(T-1)\alpha_2 M_x^2 \left(2\kappa^2 D^2 \frac{\epsilon}{pT} + \frac{8}{M^2} \epsilon^2 \right) \\
& + 2\alpha_2 M_x^2 \left(2\kappa^2 D^2 \frac{\epsilon}{pT} + \frac{8}{M^2} \epsilon^2 \right) \Bigg\}^{\frac{1}{2}}, \quad (26)
\end{aligned}$$

where $\tilde{\Phi}_\delta^* = \inf_{w \in \mathcal{U}} \tilde{\Phi}_\delta(w) > -\infty$.

Proof. Please see Appendix I. \square

Note that if the plant is fast-decaying, i.e., μ (and thus also $\mu/2\alpha_2$) is very close to 0, then

$$\frac{1}{T} \sum_{k=1}^T \mathbb{E}_{v_{[T]}} [\mathcal{G}(w_k)] \leq C_1 \sqrt{\frac{p}{\epsilon T}} + D \left(C_2 \frac{p}{\epsilon T} + 24M^2 p^2 \right)^{\frac{1}{2}}, \quad (27)$$

where C_1 and C_2 are constants. As $T \rightarrow \infty$, the right-hand side of (27) approaches $2\sqrt{6}DMP$. This nonzero upper bound mainly results from the variance of the gradient estimate (24c). It is the price to pay since we can only obtain one new evaluation of the objective function at every iteration and cannot lower the variance by increasing the sample size. The remaining terms in (26) are due to the dynamical plant being persistently excited by the proposed controller.

Remark 3. In Theorem 8, we use the average of the expected Frank-Wolfe dual gap as the convergence measure. This ergodic-type measure is similar to that investigated in Theorem 5. The interpretation is that it equals $\mathbb{E}_{v_{[T]}} [\mathcal{G}(w_R)]$, where w_R is selected uniformly at random from the candidate solutions $\{w_k\}_{k=1}^T$. Furthermore, the right-hand side of (26) is also the upper bound on $\mathbb{E}_{v_{[T]}} [\min_{k=1, \dots, T} \mathcal{G}(w_k)]$, i.e., the expected value of the minimum Frank-Wolfe dual gap, as considered in [48]. This conclusion is drawn from the following inequality

$$\begin{aligned}
\mathbb{E}_{v_{[T]}} [\min_{k=1, \dots, T} \mathcal{G}(w_k)] & \leq \mathbb{E}_{v_{[T]}} \left[\frac{1}{T} \sum_{k=1}^T \mathcal{G}(w_k) \right] \\
& = \frac{1}{T} \sum_{k=1}^T \mathbb{E}_{v_{[T]}} [\mathcal{G}(w_k)].
\end{aligned}$$

VI. NUMERICAL EVALUATIONS

We illustrate the performance of the proposed feedback controller and compare it with the first-order counterparts (i.e., feedback optimization based on gradient descent). Consider the following system

$$\begin{aligned}
x_{k+1} &= Ax_k + Bu_k + Ed, \\
y_k &= Cx_k + Dd,
\end{aligned} \quad (28)$$

where $x \in \mathbb{R}^{20}$, $u \in \mathbb{R}^{10}$, $d \in \mathbb{R}^5$ and $y \in \mathbb{R}^5$ are the state, input, disturbance and output, respectively. The elements of the system matrices in (28) are random and drawn from the standard uniform distribution. We also scale A to let its spectral radius be 0.05. The exogenous disturbance d is generated from the standard normal distribution, and its exact value is unknown beforehand. The optimization problem is given by

$$\min_{u, y} \Phi(u, y) = \underbrace{u^\top M_1 u + M_2^\top u + \|y\|^2}_{\Phi_1(u, y)} + \underbrace{\mu \|u\|_1}_{\Phi_2(u)}, \quad (29)$$

where u and y are the input and the corresponding steady-state output of the system (28), respectively. Let $M_1 = M_3^\top M_3 \in$

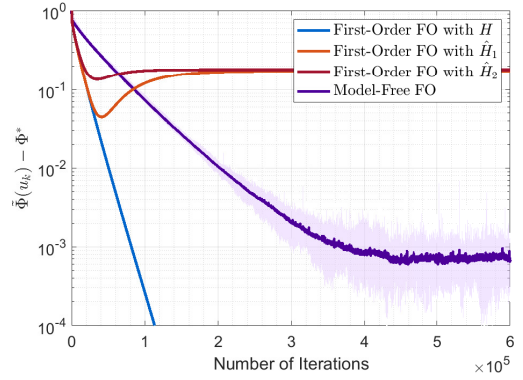


Fig. 2. Comparison between the proposed model-free feedback controller and the first-order counterparts. The bounds on the relative errors of the elements of \hat{H}_1 and \hat{H}_2 compared to those of H are 5% and 10%, respectively.

$\mathbb{R}^{10 \times 10}$ be a positive semidefinite matrix. The elements of $M_2 \in \mathbb{R}^{10}$ and $M_3 \in \mathbb{R}^{10 \times 10}$ are drawn from the standard uniform distribution. It follows that $\Phi_1(u, y)$ is a smooth convex function. For the nonsmooth regularization term $\Phi_2(u)$, we set $\mu = 10^{-3}$. Note that the ℓ_1 -norm regularization is widely used to promote the sparsity of solutions [52].

To solve general nonsmooth problems, we can apply the proposed model-free feedback controller (10) and the first-order counterpart based on sub-gradient descent. Nonetheless, to exploit the composite feature of problem (29), for both controllers, we add a proximal operator to the descent-based updates. That is, for the model-based first-order FO as comparison, we implement

$$\begin{aligned}
u_{k+1} &= \text{prox}_{\eta\Phi_2} \left(u_k - \eta \left(\nabla_u \Phi_1(u_k, y_{k+1}) \right. \right. \\
& \quad \left. \left. + H^\top \nabla_y \Phi_1(u_k, y_{k+1}) \right) \right), \quad (30)
\end{aligned}$$

where $H \triangleq C(I - A)^{-1}B$ is the steady-state input-output sensitivity of (28). For the proposed controller (10), we modify (10a) to

$$w_{k+1} = \text{prox}_{\eta\Phi_2}(w_k - \eta\tilde{\phi}_k),$$

where $\text{prox}_{\eta\Phi_2}(u)$ is the proximal operator of $\eta\Phi_2(u) = \eta\mu\|u\|_1$ and is given by

$$\text{prox}_{\eta\Phi_2}(u) = \text{sign}(u) \max\{|u| - \eta\mu, 0\}.$$

Fig. 2 illustrates the performance of the system (28) interconnected with the proposed controller and the first-order counterparts. For the proposed controller, we set the smoothing parameter $\delta = 0.001$, manually select the appropriate step size $\eta = 2.5 \times 10^{-5}$ and run 40 independent experiments. We consider the following three realizations of the first-order controller (30), i.e., with the exact sensitivity matrix H , an inexact \hat{H}_1 and an inexact \hat{H}_2 . The last two cases imitate scenarios where identification or data-driven methods are utilized to estimate H . Specifically, \hat{H}_1 and \hat{H}_2 are randomly perturbed versions of H , and the ranges of relative errors are 5% and 10%, respectively. The step sizes used in the aforementioned realizations are obtained in a binary-search-based manner and are all set as 1×10^{-4} .

In Fig. 2, the solid curve corresponding to the model-free FO represents the average trajectory of all the experiments,

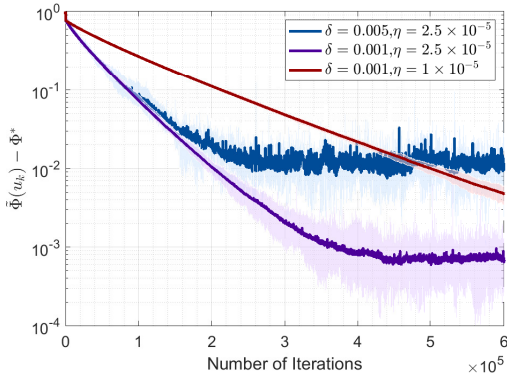


Fig. 3. Performance of the proposed model-free feedback controller with different δ and η .

and the shaded area indicates the ranges of changes of those trajectories. We observe that the first-order feedback controller based on the exact sensitivity H yields the best performance. Nonetheless, when only inexact estimations of H are available, both the convergence rates and the accuracy of solutions are severely affected. In contrast, the proposed controller robustly ensures convergence while requiring no model information. Furthermore, it is easy to implement, since no operations of identification or estimation are performed to obtain an approximate sensitivity.

Fig. 3 demonstrates the performance of the proposed feedback controller when different δ and η are used. We observe that a smaller δ leads to a narrower range of changes of trajectories and better solution accuracy. Note that δ cannot be set as an arbitrarily small number, since in that case the random direction (see (10b)) will be dominated by the measurement noises in applications. Additionally, if falling in the range that guarantees convergence, a larger step size η helps to accelerate the rate of convergence to optimality.

Next, we consider the extension to constrained inputs. In this case, we optimize the objective function $\Phi(u, y)$ in (29) over $\mathcal{U} = \{u | \underline{u} \preceq u \preceq \bar{u}\}$, where $-\underline{u}$ and \bar{u} are drawn from the standard uniform distribution. For this problem that involves the box constraint \mathcal{U} and the nonsmooth regularization, the proximal versions of the descent methods are relatively more involved (see [53]). Hence, for first-order FO with the aforementioned sensitivity matrices H , \hat{H}_1 and \hat{H}_2 , we implement the projected sub-gradient descent for its simplicity

$$u_{k+1} = \Pi_{\mathcal{U}}[u_k - \eta(\nabla_u \Phi_1(u_k, y_{k+1}) + H^\top \nabla_y \Phi_1(u_k, y_{k+1}) + \partial \Phi_2(u_k))],$$

where $\Pi_{\mathcal{U}}[\cdot]$ is the projection onto \mathcal{U} , and $\partial \Phi_2(u_k)$ is the sub-gradient of Φ_2 at u_k . Thanks to the problem setup, both $\Pi_{\mathcal{U}}[\cdot]$ and $\partial \Phi_2(u)$ have closed-form expressions. We tune the step sizes to be 7.5×10^{-5} in all these three realizations. For model-free FO, we implement both the Frank-Wolfe type update (24) and additionally (for comparison) the projected version of the descent-based update (10a), i.e.,

$$w_{k+1} = \Pi_{\mathcal{U}}[w_k - \eta \tilde{\phi}_k]. \quad (31)$$

We set the smoothing parameter δ , the step size η and the number of experiments as 0.001, 10^{-5} and 20, respectively.

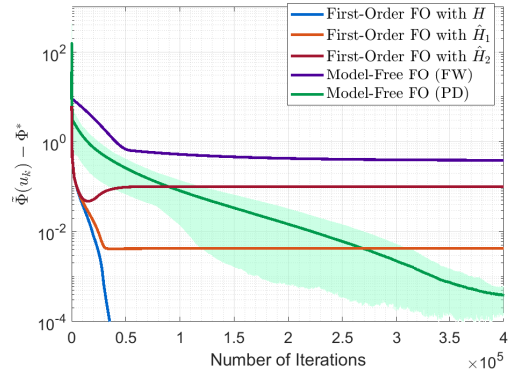


Fig. 4. Comparison between the proposed model-free feedback controller and the first-order counterparts for solving the problem with the input constraint set. Note that FW and PD refer to model-free FO based on Frank-Wolfe type updates (24) and projected descent (31), respectively.

The initial points are chosen to be $(\bar{u} + \underline{u})/2$ in all the aforementioned implementations. Fig. 4 illustrates the results of solution accuracy. We observe that the error corresponding to the model-free controller with Frank-Wolfe type updates is relatively large. The possible reason is that the performance of such a controller is more sensitive to the non-vanishing variance of the gradient estimate (10b), and further investigations are needed to improve this practical performance. For the model-free controller based on projected descent (31), the solution accuracy is better than that of the first-order feedback controllers with inexact sensitivity matrices.

In Fig. 5, we focus again on the unconstrained problem (29) and investigate the performance of different methods when the system (28) involves the time-varying disturbance d_k . In this case, the optimal solution u_k^* and the optimal value Φ_k^* of the corresponding problem (29) change due to d_k . We focus on the tracking performance in terms of u_k^* and Φ_k^* , which are measured by the error $\|u_k - u_k^*\|$ and the optimality gap $\tilde{\Phi}(u_k) - \Phi_k^*$, respectively. In every 5×10^3 iteration, the disturbance is re-drawn from the uniform distribution $U(-5 \times 10^{-3}, 5 \times 10^{-3})$. For the first-order feedback optimization controllers with the aforementioned exact H , inexact \hat{H}_1 and \hat{H}_2 , the step sizes are all tuned to be 5×10^{-4} . For the proposed controller, we set $\delta = 0.001$ and $\eta = 1 \times 10^{-4}$. Similarly, the first-order controller with the exact sensitivity enjoys the best performance. Compared to the counterpart with inexact sensitivities, the proposed controller achieves a closer tracking effect, though it features a slower convergence rate. Additionally, the feedback nature of these controllers allows the autonomous suppression of the spikes resulting from the change of d_k .

VII. CONCLUSION

We considered the problem of designing a feedback controller to steer a physical system to an efficient operating condition, which is defined by a nonconvex optimization program. The proposed discrete-time controller is model-free, thanks to the design where gradient estimates are used to update control inputs. We constructed these estimates based on current and previous evaluations of the objective function. We

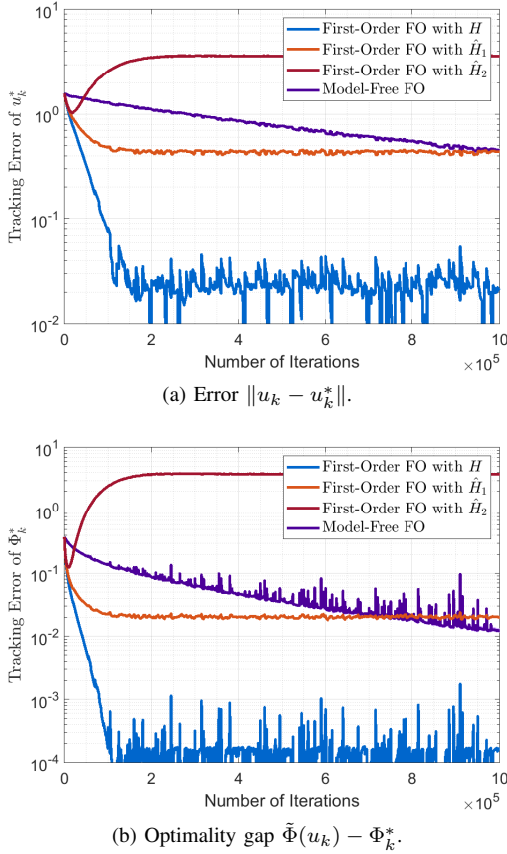


Fig. 5. Comparison of different methods in tracking the trajectory of time-varying optimal solutions.

analyzed the performance of the closed-loop interconnection of the nonlinear dynamical plant and the proposed controller. Furthermore, we established the dependence of the optimality of solutions on the problem dimension, the number of iterations, and the stability properties of the physical plant. Future directions include the systematic tuning of step sizes in online implementations, the considerations of output constraints and measurement errors, as well as the theoretical analysis of the tracking performance for time-varying problems.

APPENDIX

A. Proof of Lemma 2

Based on Assumption 3, we have

$$\begin{aligned} |e_{\Phi}(x_k, u_k)|^2 &= |\Phi(u_k, y_{k+1}) - \Phi(u_k, h(u_k, d))|^2 \\ &\leq M_y^2 \|y_{k+1} - h(u_k, d)\|^2 \\ &\leq M_y^2 M_g^2 \|x_{k+1} - x_{ss}(u_k, d)\|^2. \end{aligned}$$

It follows from (3) and (4) that

$$\begin{aligned} \|x_{k+1} - x_{ss}(u_k, d)\|^2 &\leq \frac{1}{\alpha_1} V(x_{k+1}, u_k, d) = \frac{1}{\alpha_1} V(f(x_k, u_k, d), u_k, d) \\ &\leq \frac{1}{\alpha_1} (V(x_k, u_k, d) - \alpha_3 \|x_k - x_{ss}(u_k, d)\|^2) \\ &\leq \frac{1}{\alpha_1} \left(1 - \frac{\alpha_3}{\alpha_2}\right) V(x_k, u_k, d). \end{aligned} \quad (32)$$

Hence, based on the definition (5) of μ , inequality (11) holds.

B. Proof of Lemma 3

Based on (3), we have

$$\begin{aligned} V(x_k, u_k, d) &\leq \alpha_2 \|x_k - x_{ss}(u_k, d)\|^2 \\ &= \alpha_2 \|x_k - x_{ss}(u_{k-1}, d) + x_{ss}(u_{k-1}, d) - x_{ss}(u_k, d)\|^2 \\ &\stackrel{(s.1)}{\leq} 2\alpha_2 (\|x_k - x_{ss}(u_{k-1}, d)\|^2 + \|x_{ss}(u_{k-1}, d) - x_{ss}(u_k, d)\|^2) \\ &\stackrel{(s.2)}{\leq} 2\alpha_2 \left(\frac{1}{\alpha_1} \left(1 - \frac{\alpha_3}{\alpha_2}\right) V(x_{k-1}, u_{k-1}, d) + M_x^2 \|u_k - u_{k-1}\|^2\right), \end{aligned}$$

where (s.1) follows from the inequality $\|a + b\|^2 \leq 2(\|a\|^2 + \|b\|^2)$, $\forall a, b$, and (s.2) is built on (32) and the Lipschitz continuity of $x_{ss}(u, d)$. By taking expectation of both sides of the above inequality with respect to $v_{[k]}$ and using the definition (5) of μ , we obtain

$$\begin{aligned} \mathbb{E}_{v_{[k]}}[V(x_k, u_k, d)] &\leq \mu \mathbb{E}_{v_{[k]}}[V(x_{k-1}, u_{k-1}, d)] \\ &\quad + 2\alpha_2 M_x^2 \mathbb{E}_{v_{[k]}}[\|u_k - u_{k-1}\|^2]. \end{aligned} \quad (33)$$

The bound on $\mathbb{E}_{v_{[k]}}[\|u_k - u_{k-1}\|^2]$ is given by

$$\begin{aligned} \mathbb{E}_{v_{[k]}}[\|u_k - u_{k-1}\|^2] &= \mathbb{E}_{v_{[k]}}[\|w_k - w_{k-1} + \delta v_k - \delta v_{k-1}\|^2] \\ &\stackrel{(s.1)}{\leq} \mathbb{E}_{v_{[k]}}[2\|w_k - w_{k-1}\|^2 + 2\delta^2 \|v_k - v_{k-1}\|^2] \\ &\stackrel{(s.2)}{\leq} 2\eta^2 \mathbb{E}_{v_{[k]}}[\|\tilde{\phi}_{k-1}\|^2] + 4\delta^2 p, \end{aligned}$$

where (s.1) follows by $\mathbb{E}[(a + b)^2] \leq 2\mathbb{E}[a^2 + b^2]$, $\forall a, b$; (s.2) relies on the independence between v_k and v_{k-1} , and $\mathbb{E}[v] = 0$, $\mathbb{E}[\|v\|^2] = p$, $\forall v \sim \mathcal{N}(0, I)$, see Lemma 9 below. Hence, the inequality (12) holds.

C. Proof of Lemma 4

First, we present a lemma proved in [38] for the upper bounds on the moments of standard normal random vectors.

Lemma 9 ([38, Lemma 1]). *Let $v \in \mathbb{R}^p$ satisfy the standard multivariate normal distribution. Then,*

$$\mathbb{E}[\|v\|^t] \leq \begin{cases} p^{t/2}, & \text{if } t \in [0, 2], \\ (p + t)^{t/2}, & \text{if } t > 2. \end{cases}$$

Two special cases include $\mathbb{E}[\|v\|^2] = p$ and $\mathbb{E}[\|v\|^4] \leq (p + 4)^2$, $\forall v \sim \mathcal{N}(0, I_{p \times p})$.

Then, we focus on the bound for $\mathbb{E}_{v_{[k]}}[\|\tilde{\phi}_k\|^2]$. Based on (10b), we have

$$\begin{aligned} \mathbb{E}_{v_{[k]}}[\|\tilde{\phi}_k\|^2] &= \frac{1}{\delta^2} \mathbb{E}_{v_{[k]}}[\|v_k(\Phi(u_k, y_{k+1}) - \Phi(u_{k-1}, y_k))\|^2] \\ &= \frac{1}{\delta^2} \mathbb{E}_{v_{[k]}}[\|v_k(\tilde{\Phi}(u_k) - \tilde{\Phi}(u_{k-1})) \\ &\quad + v_k(e_{\Phi}(x_k, u_k) - e_{\Phi}(x_{k-1}, u_{k-1}))\|^2] \\ &\stackrel{(s.1)}{\leq} \underbrace{\frac{3}{\delta^2} \mathbb{E}_{v_{[k]}}[\|v_k(\tilde{\Phi}(u_k) - \tilde{\Phi}(u_{k-1}))\|^2]}_{\textcircled{1}} \\ &\quad + \underbrace{\frac{3}{\delta^2} \mathbb{E}_{v_{[k]}}[\|v_k e_{\Phi}(x_k, u_k)\|^2]}_{\textcircled{2}} + \underbrace{\frac{3}{\delta^2} \mathbb{E}_{v_{[k]}}[\|v_k e_{\Phi}(x_{k-1}, u_{k-1})\|^2]}_{\textcircled{3}}, \end{aligned} \quad (34)$$

where (s.1) follows from the fact that $\forall a, b, c, \mathbb{E}[(a+b+c)^2] \leq 3\mathbb{E}[a^2 + b^2 + c^2] = 3\mathbb{E}[a^2] + 3\mathbb{E}[b^2] + 3\mathbb{E}[c^2]$.

First, we provide a bound on term ① in (34).

$$\begin{aligned}
\textcircled{1} &= \frac{3}{\delta^2} \mathbb{E}_{v_{[k]}} [\|v_k(\tilde{\Phi}(w_k + \delta v_k) - \tilde{\Phi}(w_{k-1} + \delta v_k))\|^2 \\
&\quad + \|\tilde{\Phi}(w_{k-1} + \delta v_k) - \tilde{\Phi}(w_{k-1} + \delta v_{k-1})\|^2] \\
&\stackrel{(s.1)}{=} \frac{6}{\delta^2} \mathbb{E}_{v_{[k]}} [\|v_k(\tilde{\Phi}(w_k + \delta v_k) - \tilde{\Phi}(w_{k-1} + \delta v_k))\|^2 \\
&\quad + \|v_k(\tilde{\Phi}(w_{k-1} + \delta v_k) - \tilde{\Phi}(w_{k-1} + \delta v_{k-1}))\|^2] \\
&\stackrel{(s.2)}{\leq} \frac{6M^2}{\delta^2} \mathbb{E}_{v_{[k]}} [\|w_k - w_{k-1}\|^2 \|v_k\|^2 \\
&\quad + \delta^2 \|v_k - v_{k-1}\|^2 \|v_k\|^2] \\
&\stackrel{(s.3)}{\leq} \frac{6M^2}{\delta^2} (\eta^2 \mathbb{E}_{v_{[k]}} [\|\tilde{\phi}_{k-1}\|^2] \mathbb{E}_{v_{[k]}} [\|v_k\|^2] \\
&\quad + \delta^2 \mathbb{E}_{v_{[k]}} [2(\|v_k\|^2 + \|v_{k-1}\|^2) \|v_k\|^2]) \\
&\stackrel{(s.4)}{\leq} \frac{6}{\delta^2} M^2 \eta^2 p \mathbb{E}_{v_{[k]}} [\|\tilde{\phi}_{k-1}\|^2] + 24M^2(p+4)^2,
\end{aligned}$$

where (s.1) relies on the fact that $\mathbb{E}[(a+b)^2] \leq 2\mathbb{E}[a^2 + b^2]$, $\forall a, b$; (s.2) follows from the assumption that $\tilde{\Phi}(u)$ is M -Lipschitz continuous; (s.3) utilizes the independence between v_k and $-\eta\tilde{\phi}_{k-1}$ and the inequality $\|a-b\|^2 \leq 2(\|a\|^2 + \|b\|^2)$, $\forall a, b$; (s.4) follows by Lemma 9 and the independence between v_k and v_{k-1} .

Then, we bound term ② in (34).

$$\begin{aligned}
\textcircled{2} &= \frac{3}{\delta^2} \mathbb{E}_{v_{[k]}} [\|v_k\|^2 \cdot |e_{\Phi}(x_k, u_k)|^2] \\
&\stackrel{(s.1)}{\leq} \frac{3}{\delta^2} (\mathbb{E}_{v_{[k]}} [\|v_k\|^4])^{\frac{1}{2}} (\mathbb{E}_{v_{[k]}} [|e_{\Phi}(x_k, u_k)|^4])^{\frac{1}{2}} \\
&\stackrel{(s.2)}{\leq} (p+4) \frac{3M_y^2 M_g^2}{\alpha_1 \delta^2} \left(1 - \frac{\alpha_3}{\alpha_2}\right) \mathbb{E}_{v_{[k]}} [V(x_k, u_k, d)],
\end{aligned}$$

where (s.1) relies on the Cauchy-Schwarz inequality, and its motivation is to split the product of two correlated random variables and then use the corresponding upper bounds; (s.2) follows by Lemma 9 and the bound on $|e_{\Phi}(x_k, u_k)|^4$ acquired by squaring both sides of (11).

Finally, we bound term ③ in (34).

$$\begin{aligned}
\textcircled{3} &\stackrel{(s.1)}{=} \frac{3}{\delta^2} \mathbb{E}_{v_{[k]}} [\|v_k\|^2] \mathbb{E}_{v_{[k]}} [|e_{\Phi}(x_{k-1}, u_{k-1})|^2] \\
&\stackrel{(s.2)}{\leq} \frac{3pM_y^2 M_g^2}{\alpha_1 \delta^2} \left(1 - \frac{\alpha_3}{\alpha_2}\right) \mathbb{E}_{v_{[k]}} [V(x_{k-1}, u_{k-1}, d)],
\end{aligned}$$

where (s.1) follows from the independence between v_k and $e_{\Phi}(x_{k-1}, u_{k-1})$; (s.2) follows by Lemma 9 and the bound on $|e_{\Phi}(x_k, u_k)|^2$ in (11).

By combining the obtained upper bounds and using the definition (5) of μ , we arrive at (13).

D. A Bound on an Intermediate Term

We establish a bound on the term $\mathbb{E}_{v_{[k]}} [-\nabla \tilde{\Phi}_{\delta}^{\top}(w_k) \tilde{\phi}_k]$, which is useful for characterizing the optimality of the steady state of the interconnection of (10) and (1).

Lemma 10. *If Assumptions 1 and 3 hold, with (10), we have*

$$\begin{aligned}
\mathbb{E}_{v_{[k]}} [-\nabla \tilde{\Phi}_{\delta}^{\top}(w_k) \tilde{\phi}_k] &\leq -\frac{1}{2} \mathbb{E}_{v_{[k]}} [\|\nabla \tilde{\Phi}_{\delta}(w_k)\|^2] \\
&\quad + \frac{pM_y^2 M_g^2}{2\delta^2 \alpha_1} \left(1 - \frac{\alpha_3}{\alpha_2}\right) \mathbb{E}_{v_{[k]}} [V(x_k, u_k, d)].
\end{aligned} \tag{35}$$

Proof. Note that

$$\begin{aligned}
\mathbb{E}_{v_{[k]}} [-\nabla \tilde{\Phi}_{\delta}^{\top}(w_k) \tilde{\phi}_k] &\stackrel{(s.1)}{=} \mathbb{E}_{v_{[k-1]}} [\mathbb{E}_{v_k} [-\nabla \tilde{\Phi}_{\delta}^{\top}(w_k) \tilde{\phi}_k | v_{[k-1]}]] \\
&\stackrel{(s.2)}{=} \mathbb{E}_{v_{[k-1]}} [\nabla \tilde{\Phi}_{\delta}^{\top}(w_k) \mathbb{E}_{v_k} [-\tilde{\phi}_k | v_{[k-1]}]],
\end{aligned} \tag{36}$$

where (s.1) follows from the tower rule; (s.2) holds since $\tilde{\Phi}_{\delta}(w_k)$ is measurable with respect to $v_{[k-1]}$. Next, we focus on $\mathbb{E}_{v_k} [-\tilde{\phi}_k | v_{[k-1]}]$.

$$\begin{aligned}
\mathbb{E}_{v_k} [-\tilde{\phi}_k | v_{[k-1]}] &= \mathbb{E}_{v_k} \left[-\frac{v_k}{\delta} (\tilde{\Phi}(u_k) + e_{\Phi}(x_k, u_k)) | v_{[k-1]} \right] \\
&\quad + \mathbb{E}_{v_k} \left[\frac{v_k}{\delta} (\tilde{\Phi}(u_{k-1}) + e_{\Phi}(x_{k-1}, u_{k-1})) | v_{[k-1]} \right] \\
&\stackrel{(s.1)}{=} \mathbb{E}_{v_k} \left[-\frac{v_k}{\delta} \tilde{\Phi}(w_k + \delta v_k) | v_{[k-1]} \right] \\
&\quad + \mathbb{E}_{v_k} \left[-\frac{v_k}{\delta} e_{\Phi}(x_k, u_k) | v_{[k-1]} \right] \\
&\stackrel{(s.2)}{=} -\nabla \tilde{\Phi}_{\delta}(w_k) + \mathbb{E}_{v_k} \left[-\frac{v_k}{\delta} e_{\Phi}(x_k, u_k) | v_{[k-1]} \right],
\end{aligned} \tag{37}$$

where (s.1) follows by the independence of $\tilde{\Phi}(u_{k-1})$ and $e_{\Phi}(x_{k-1}, u_{k-1})$ on v_k and $\mathbb{E}_{v_k}[v_k] = 0$; (s.2) utilizes [38, Eq. (21)] (see also [42, Lemma 3.1]). By plugging (37) into (36) and utilizing the inequality $\forall z_1, z_2, \mathbb{E}[z_1^{\top} z_2] \leq (\mathbb{E}[\|z_1\|^2] \mathbb{E}[\|z_2\|^2])^{\frac{1}{2}} \leq \frac{1}{2}(\mathbb{E}[\|z_1\|^2] + \mathbb{E}[\|z_2\|^2])$, we obtain

$$\begin{aligned}
\mathbb{E}_{v_{[k]}} [-\nabla \tilde{\Phi}_{\delta}^{\top}(w_k) \tilde{\phi}_k] &= -\mathbb{E}_{v_{[k]}} [\|\nabla \tilde{\Phi}_{\delta}(w_k)\|^2] \\
&\quad + \mathbb{E}_{v_{[k-1]}} \left[\nabla \tilde{\Phi}_{\delta}^{\top}(w_k) \mathbb{E}_{v_k} \left[-\frac{v_k}{\delta} e_{\Phi}(x_k, u_k) | v_{[k-1]} \right] \right] \\
&\leq -\mathbb{E}_{v_{[k]}} [\|\nabla \tilde{\Phi}_{\delta}(w_k)\|^2] + \frac{1}{2} \mathbb{E}_{v_{[k-1]}} [\|\nabla \tilde{\Phi}_{\delta}(w_k)\|^2] \\
&\quad + \frac{1}{2} \mathbb{E}_{v_{[k-1]}} \left[\left\| \mathbb{E}_{v_k} \left[\frac{v_k}{\delta} e_{\Phi}(x_k, u_k) | v_{[k-1]} \right] \right\|^2 \right].
\end{aligned} \tag{38}$$

For the last term of the right-hand side of (38), we have

$$\begin{aligned}
\mathbb{E}_{v_{[k-1]}} \left[\left\| \mathbb{E}_{v_k} \left[\frac{v_k}{\delta} e_{\Phi}(x_k, u_k) | v_{[k-1]} \right] \right\|^2 \right] &\stackrel{(s.1)}{=} \mathbb{E}_{v_{[k-1]}} \left[\sum_{j=1}^p \frac{1}{\delta^2} \mathbb{E}_{v_k}^2 [e_{\Phi}(x_k, u_k) v_k(j) | v_{[k-1]}] \right] \\
&\stackrel{(s.2)}{\leq} \frac{1}{\delta^2} \mathbb{E}_{v_{[k-1]}} \left[\sum_{j=1}^p \mathbb{E}_{v_k} [e_{\Phi}^2(x_k, u_k) | v_{[k-1]}] \mathbb{E}_{v_k} [v_k^2(j) | v_{[k-1]}] \right] \\
&\stackrel{(s.3)}{=} \frac{p}{\delta^2} \mathbb{E}_{v_{[k-1]}} [\mathbb{E}_{v_k} [e_{\Phi}^2(x_k, u_k) | v_{[k-1]}]] \\
&\stackrel{(s.4)}{\leq} \frac{pM_y^2 M_g^2}{\delta^2 \alpha_1} \left(1 - \frac{\alpha_3}{\alpha_2}\right) \mathbb{E}_{v_{[k]}} [V(x_k, u_k, d)],
\end{aligned} \tag{39}$$

where in (s.1), $v_k(j)$ denotes the j -th component of v_k ; (s.2) follows from the Cauchy-Schwarz inequality; (s.3) uses $\mathbb{E}_{v_k}[v_k^2(j)] = 1, \forall v_k(j) \sim \mathcal{N}(0, 1)$; (s.4) relies on (11) and the tower rule. By combining (39) with (38), we obtain (35). \square

E. An Auxiliary Lemma

The following auxiliary lemma gives the bounds on the partial sums of two coupled sequences of nonnegative numbers, and is inspired by [30, Proof of Theorem 1]. Let $(g_k)_{k \in \mathbb{N}}$ and $(h_k)_{k \in \mathbb{N}}$ be two nonnegative sequences that satisfy

$$g_k \leq a_1 g_{k-1} + b_1 h_{k-1} + d_1, \quad (40a)$$

$$h_k \leq a_2 g_{k-1} + b_2 h_{k-1} + d_2. \quad (40b)$$

Suppose that the matrix of coefficients C satisfies

$$C = \begin{bmatrix} a_1 & b_1 \\ a_2 & b_2 \end{bmatrix}, \quad \|C\| = \sigma_{\max}(C) \triangleq \sigma < 1, \quad (41)$$

Let the T -th partial sums of $(g_k)_{k \in \mathbb{N}}$ and $(h_k)_{k \in \mathbb{N}}$ be denoted by

$$G_T = \sum_{k=0}^T g_k, \quad H_T = \sum_{k=0}^T h_k,$$

respectively. The bounds on G_T and H_T are provided in the following lemma.

Lemma 11. *With nonnegative sequences (40) and the matrix of coefficients (41), we have*

$$\max\{G_T, H_T\} \leq \left(\sigma^T + \frac{1}{1-\sigma}\right)(g_0 + h_0) + \frac{T}{1-\sigma}(d_1 + d_2). \quad (42)$$

Proof. By summing over both sides of (40) when $k = T, T-1, \dots, 1$, we have

$$\begin{aligned} G_T - g_0 &\leq a_1 G_{T-1} + b_1 H_{T-1} + T d_1, \\ H_T - h_0 &\leq a_2 G_{T-1} + b_2 H_{T-1} + T d_2, \end{aligned}$$

which can be compactly written as

$$\begin{bmatrix} G_T \\ H_T \end{bmatrix} \leq C \begin{bmatrix} G_{T-1} \\ H_{T-1} \end{bmatrix} + \begin{bmatrix} T d_1 + g_0 \\ T d_2 + h_0 \end{bmatrix}.$$

By recursively using the above inequality, we have

$$\begin{bmatrix} G_T \\ H_T \end{bmatrix} \leq C^T \begin{bmatrix} g_0 \\ h_0 \end{bmatrix} + \sum_{k=1}^T C^{T-k} \begin{bmatrix} k d_1 + g_0 \\ k d_2 + h_0 \end{bmatrix}.$$

Note that G_T and H_T are nonnegative for any $T \in \mathbb{N}$. It follows that

$$\begin{aligned} \max\{G_T, H_T\} &\leq \left\| \begin{bmatrix} G_T \\ H_T \end{bmatrix} \right\| \\ &\stackrel{(s.1)}{\leq} \sigma^T \left\| \begin{bmatrix} g_0 \\ h_0 \end{bmatrix} \right\| + \sum_{k=1}^T \sigma^{T-k} \left\| \begin{bmatrix} T d_1 + g_0 \\ T d_2 + h_0 \end{bmatrix} \right\| \\ &\stackrel{(s.2)}{\leq} \sigma^T (g_0 + h_0) + \frac{1}{1-\sigma} (T(d_1 + d_2) + g_0 + h_0), \end{aligned}$$

where (s.1) relies on the sub-multiplicativity of the norms and $\|C\| = \sigma$; (s.2) follows from the fact that $\|[a \ b]^\top\| \leq a + b$ for any nonnegative numbers a and b . Hence, (42) holds. \square

F. Proof of Theorem 5

It follows from Assumption 3 that the Gaussian smooth approximation $\tilde{\Phi}_\delta(w)$ is $M\sqrt{p}/\delta$ ($\triangleq L$)-smooth. Hence,

$$\begin{aligned} \tilde{\Phi}_\delta(w_{k+1}) &\leq \tilde{\Phi}_\delta(w_k) + \nabla \tilde{\Phi}_\delta^\top(w_k)(w_{k+1} - w_k) + \frac{L}{2} \|w_{k+1} - w_k\|^2 \\ &= \tilde{\Phi}_\delta(w_k) - \eta \nabla \tilde{\Phi}_\delta^\top(w_k) \tilde{\phi}_k + \frac{L\eta^2}{2} \|\tilde{\phi}_k\|^2. \end{aligned} \quad (43)$$

By taking expectations of both sides of (43) with respect to $v_{[k]}$ and referring to Lemma 10 in Appendix D, we have

$$\begin{aligned} \mathbb{E}_{v_{[k]}}[\tilde{\Phi}_\delta(w_{k+1})] &\leq \mathbb{E}_{v_{[k]}}[\tilde{\Phi}_\delta(w_k)] - \frac{\eta}{2} \mathbb{E}_{v_{[k]}}[\|\nabla \tilde{\Phi}_\delta(w_k)\|^2] \\ &\quad + \frac{\eta p M_y^2 M_g^2}{2\delta^2 \alpha_1} \left(1 - \frac{\alpha_3}{\alpha_2}\right) \mathbb{E}_{v_{[k]}}[V(x_k, u_k, d)] \\ &\quad + \frac{L\eta^2}{2} \mathbb{E}_{v_{[k]}}[\|\tilde{\phi}_k\|^2]. \end{aligned}$$

By rearranging terms and telescoping sums, we obtain

$$\begin{aligned} &\sum_{k=0}^{T-1} \mathbb{E}_{v_{[T-1]}}[\|\nabla \tilde{\Phi}_\delta(w_k)\|^2] \\ &\leq \frac{2}{\eta} \left(\mathbb{E}_{v_{[T-1]}}[\tilde{\Phi}_\delta(w_0)] - \mathbb{E}_{v_{[T-1]}}[\tilde{\Phi}_\delta(w_T)] \right) \\ &\quad + L\eta \sum_{k=0}^{T-1} \mathbb{E}_{v_{[T-1]}}[\|\tilde{\phi}_k\|^2] \\ &\quad + \frac{p M_y^2 M_g^2}{\delta^2 \alpha_1} \left(1 - \frac{\alpha_3}{\alpha_2}\right) \sum_{k=0}^{T-1} \mathbb{E}_{v_{[T-1]}}[V(x_k, u_k, d)]. \end{aligned} \quad (44)$$

We now focus on the last two terms of (44). By incorporating (12) into the right-hand side of (13), we have

$$\begin{bmatrix} \mathbb{E}_{v_{[k]}}[\|\tilde{\phi}_k\|^2] \\ \mathbb{E}_{v_{[k]}}[V(x_k, u_k, d)] \end{bmatrix} \preceq C \begin{bmatrix} \mathbb{E}_{v_{[k]}}[\|\tilde{\phi}_{k-1}\|^2] \\ \mathbb{E}_{v_{[k]}}[V(x_{k-1}, u_{k-1}, d)] \end{bmatrix} + \begin{bmatrix} d_1 \\ d_2 \end{bmatrix},$$

where $C = \begin{bmatrix} c_{11} & c_{12} \\ c_{21} & c_{22} \end{bmatrix}$ and

$$\begin{aligned} c_{11} &= \frac{6\eta^2}{\delta^2} \left(M^2 p + 2M_y^2 M_g^2 M_x^2 (p+4) \frac{\alpha_2}{\alpha_1} \left(1 - \frac{\alpha_3}{\alpha_2}\right) \right), \\ c_{12} &= \frac{3M_y^2 M_g^2}{\alpha_1 \delta^2} \left(1 - \frac{\alpha_3}{\alpha_2}\right) \left[p + (p+4) \frac{2\alpha_2}{\alpha_1} \left(1 - \frac{\alpha_3}{\alpha_2}\right) \right], \\ c_{21} &= 4\alpha_2 \eta^2 M_x^2, \\ c_{22} &= \frac{2\alpha_2}{\alpha_1} \left(1 - \frac{\alpha_3}{\alpha_2}\right), \\ d_1 &= 24M^2 (p+4)^2 + 24M_y^2 M_g^2 M_x^2 p (p+4) \frac{\alpha_2}{\alpha_1} \left(1 - \frac{\alpha_3}{\alpha_2}\right), \\ d_2 &= 8\alpha_2 p \delta^2 M_x^2. \end{aligned} \quad (45)$$

The above inequality can be reformulated as

$$\begin{bmatrix} \mathbb{E}_{v_{[k]}}[\|\tilde{\phi}_k\|^2] \\ \mathbb{E}_{v_{[k]}} \left[\sqrt{\frac{c_{12}}{c_{21}}} V(x_k, u_k, d) \right] \end{bmatrix} \preceq C' \begin{bmatrix} \mathbb{E}_{v_{[k]}}[\|\tilde{\phi}_{k-1}\|^2] \\ \mathbb{E}_{v_{[k]}} \left[\sqrt{\frac{c_{12}}{c_{21}}} V(x_{k-1}, u_{k-1}, d) \right] \end{bmatrix} + \begin{bmatrix} d_1 \\ \sqrt{\frac{c_{12}}{c_{21}}} d_2 \end{bmatrix},$$

where the elements of C' are given by

$$c'_{11} = c_{11}, \quad c'_{12} = c'_{21} = \sqrt{c_{12}c_{21}}, \quad c'_{22} = c_{22}. \quad (46)$$

Since C' is a symmetric matrix, its spectral norm is $\|C'\| = \rho(C') \triangleq \rho$. Additionally, C' is a positive matrix. It follows from the Perron-Frobenius theorem [54] that ρ equals to the Perron eigenvalue of C' . Hence,

$$\begin{aligned} \rho &= \frac{c'_{11} + c'_{22}}{2} + \sqrt{\left(\frac{c'_{11} - c'_{22}}{2}\right)^2 + c'_{12}c'_{21}} \\ &\leq \frac{c'_{11} + c'_{22}}{2} + \left|\frac{c'_{11} - c'_{22}}{2}\right| + \sqrt{c'_{12}c'_{21}} \\ &= \max\{c'_{11}, c'_{22}\} + \sqrt{c'_{12}c'_{21}}. \end{aligned}$$

Therefore, to guarantee that $\rho < 1$, we need to set δ and η such that

$$c'_{11} + \sqrt{c'_{12}c'_{21}} < 1, \quad c'_{22} + \sqrt{c'_{12}c'_{21}} < 1. \quad (47)$$

Note that $\mathbb{E}_{v_{[k]}}[\|\tilde{\phi}_k\|^2]$ and $\mathbb{E}_{v_{[k]}}[\sqrt{c_{12}/c_{21}}V(x_k, u_k, d)]$ are non-negative for any $k \in \mathbb{N}$. Hence, from Lemma 11 in Appendix E, we have

$$\begin{aligned} &\max\left\{\sum_{k=0}^{T-1} \mathbb{E}_{v_{[T-1]}}[\|\tilde{\phi}_k\|^2], \sum_{k=0}^{T-1} \mathbb{E}_{v_{[T-1]}}[\sqrt{\frac{c_{12}}{c_{21}}}V(x_k, u_k, d)]\right\} \\ &\leq \left(\rho^{T-1} + \frac{1}{1-\rho}\right)B_0 + \frac{T-1}{1-\rho}(d_1 + \sqrt{\frac{c_{12}}{c_{21}}}d_2), \end{aligned} \quad (48)$$

where $B_0 = \mathbb{E}[\|\tilde{\phi}(w_0)\|^2] + \mathbb{E}[\sqrt{c_{12}/c_{21}}V(x_0, u_0, d)]$. By combining (48) with (44) and dividing both sides of the inequality by T , we have

$$\begin{aligned} &\frac{1}{T} \sum_{k=0}^{T-1} \mathbb{E}_{v_{[T-1]}}[\|\nabla\tilde{\Phi}_\delta(w_k)\|^2] \leq \frac{2}{\eta T} (\mathbb{E}[\tilde{\Phi}_\delta(w_0)] - \tilde{\Phi}_\delta^*) \\ &+ \frac{1}{T} \left(\frac{\eta M \sqrt{p}}{\delta} + \frac{p M_y^2 M_g^2}{\delta^2 \alpha_1} \sqrt{\frac{c_{21}}{c_{12}}} \left(1 - \frac{\alpha_3}{\alpha_2}\right) \right) \\ &\cdot \left[\left(\rho^{T-1} + \frac{1}{1-\rho}\right)B_0 + \frac{T-1}{1-\rho}(d_1 + \sqrt{\frac{c_{12}}{c_{21}}}d_2) \right], \end{aligned} \quad (49)$$

where we use the fact that $\mathbb{E}[\tilde{\Phi}_\delta(w_T)] \geq \tilde{\Phi}_\delta^* \triangleq \inf_{u \in \mathbb{R}^p} \tilde{\Phi}_\delta(u)$. Note that $\tilde{\Phi}_\delta^*$ is finite, since $\inf_{u \in \mathbb{R}^p} \tilde{\Phi}(u)$ is finite (see Assumption 3) and $\tilde{\Phi}_\delta(u)$ is close to $\tilde{\Phi}(u)$ (see Lemma 1).

To ensure that $|\tilde{\Phi}_\delta(u) - \tilde{\Phi}(u)| \leq \epsilon$, we set $\delta = \frac{\epsilon}{M \sqrt{p}}$. With direct calculations, we obtain that the following terms are of the orders of

- i. $\sqrt{\frac{c_{12}}{c_{21}}} = \mathcal{O}\left(\frac{p}{\eta \epsilon} \left(\frac{1}{\alpha_1 \alpha_2} \left(1 - \frac{\alpha_3}{\alpha_2}\right)\right)^{\frac{1}{2}}\right),$
- ii. $\frac{\eta M \sqrt{p}}{\delta} + \frac{p M_y^2 M_g^2}{\delta^2 \alpha_1} \sqrt{\frac{c_{21}}{c_{12}}} \left(1 - \frac{\alpha_3}{\alpha_2}\right) = \mathcal{O}\left(\frac{p \eta}{\epsilon}\right),$
- iii. $\left(\rho^{T-1} + \frac{1}{1-\rho}\right)B_0 + \frac{T-1}{1-\rho}(d_1 + \sqrt{\frac{c_{12}}{c_{21}}}d_2) = \mathcal{O}\left(\frac{p}{1-\rho} \left(Tp + \frac{T\epsilon + \frac{1}{\epsilon \alpha_2}}{\eta} \left(\frac{\alpha_2}{\alpha_1} \left(1 - \frac{\alpha_3}{\alpha_2}\right)\right)^{\frac{1}{2}}\right)\right).$

Let $\eta = \frac{\kappa \sqrt{\epsilon}}{p^{\frac{3}{2}} \sqrt{T}}$ such that $\frac{1}{\eta T}$ and $\frac{p^3 \eta}{\epsilon}$ are of the same order. Then, based on the definition (5) of μ , the upper bound on the right-hand side of (49) is of the order of

$$\mathcal{O}\left(\frac{p^{\frac{3}{2}}}{\sqrt{\epsilon T}(1-\rho)}\right) + \mathcal{O}\left(\frac{p^2}{1-\rho} \cdot \left(1 + \frac{1}{T \epsilon^2 \alpha_2}\right) \cdot \sqrt{\mu}\right).$$

The parameter κ is set to meet the requirement (47), i.e.,

$$\begin{aligned} \zeta_1 \kappa^2 + \zeta_2 \kappa &< 1, \\ \zeta_3 + \zeta_2 \kappa &< 1. \end{aligned} \quad (50)$$

where

$$\begin{aligned} \zeta_1 &= \frac{6M^2}{p^2 T \epsilon} \left(M^2 p + 2M_y^2 M_g^2 M_x^2 (p+4) \frac{\alpha_2}{\alpha_1} \left(1 - \frac{\alpha_3}{\alpha_2}\right) \right), \\ \zeta_2 &= \left(\frac{12\alpha_2 M^2 M_x^2 M_y^2 M_g^2}{\alpha_1 p^2 T \epsilon} \left(1 - \frac{\alpha_3}{\alpha_2}\right) \left[p + (p+4) \frac{2\alpha_2}{\alpha_1} \left(1 - \frac{\alpha_3}{\alpha_2}\right) \right] \right)^{\frac{1}{2}}, \\ \zeta_3 &= \frac{2\alpha_2}{\alpha_1} \left(1 - \frac{\alpha_3}{\alpha_2}\right). \end{aligned}$$

The feasible range is denoted by $(0, \kappa^*)$. It is nonempty provided that $\zeta_3 < 1$ (see Assumption 2). Based on (50), the parametric conditions, and the definition (5) of μ , we have

$$\begin{aligned} \kappa^* &= \min \left\{ \frac{-\zeta_2 + \sqrt{\zeta_2^2 + 4\zeta_1}}{2\zeta_1}, \frac{1 - \zeta_3}{\zeta_2} \right\} \\ &= \mathcal{O}\left(\min \left\{ 1 - \sqrt{\mu}, \frac{1 - \mu}{\sqrt{\mu}} \right\} \cdot \sqrt{p T \epsilon}\right), \\ \rho &= \max \{ \zeta_1 \kappa^2, \zeta_3 \} + \zeta_2 \kappa \\ &= \mathcal{O}\left(\max \left(\frac{1}{T p \epsilon}, \mu \right) + \left(\frac{\mu}{T p \epsilon} \right)^{\frac{1}{2}}\right). \end{aligned}$$

G. Proof of Corollary 1

The bound on $\|\nabla\tilde{\Phi}_\delta(u_k)\|^2$ is given by

$$\begin{aligned} \|\nabla\tilde{\Phi}_\delta(u_k)\|^2 &\stackrel{(s.1)}{\leq} 2(\|\nabla\tilde{\Phi}_\delta(w_k)\|^2 + \|\nabla\tilde{\Phi}_\delta(w_k) - \nabla\tilde{\Phi}_\delta(u_k)\|^2) \\ &\stackrel{(s.2)}{\leq} 2(\|\nabla\tilde{\Phi}_\delta(w_k)\|^2 + \left(\frac{M\sqrt{p}}{\delta}\delta\|v_k\|\right)^2) \\ &\leq 2(\|\nabla\tilde{\Phi}_\delta(w_k)\|^2 + M^2 p \|v_k\|^2), \end{aligned} \quad (51)$$

where (s.1) follows by the inequality $\forall a, b, \|b\|^2 = \|a - (a - b)\|^2 \leq 2(\|a\|^2 + \|a - b\|^2)$; (s.2) uses the property that $\nabla\tilde{\Phi}_\delta(u)$ is $M\sqrt{p}/\delta$ -Lipschitz. By taking expectations of both sides of (51) with respect to $v_{[T-1]}$, we obtain

$$\begin{aligned} &\mathbb{E}_{v_{[T-1]}}[\|\nabla\tilde{\Phi}_\delta(u_k)\|^2] \\ &\leq 2(\mathbb{E}_{v_{[T-1]}}[\|\nabla\tilde{\Phi}_\delta(w_k)\|^2] + M^2 p \mathbb{E}_{v_{[T-1]}}[\|v_k\|^2]) \\ &= 2\mathbb{E}_{v_{[T-1]}}[\|\nabla\tilde{\Phi}_\delta(w_k)\|^2] + 2M^2 p^2, \end{aligned}$$

where the last equality is due to $\mathbb{E}[\|v_k\|^2] = p, \forall v_k \sim \mathcal{N}(0, I_{p \times p})$. It follows that (16) holds.

H. Proof of Theorem 6

Note that

$$\frac{1}{T} \sum_{k=1}^{T-1} \mathbb{E}_{v_{[T-1]}}[\|x_{k+1} - x_{ss}(u_k, d)\|^2]$$

$$\begin{aligned}
&\stackrel{(s.1)}{\leq} \frac{\mu}{2\alpha_2 T} \sum_{k=1}^{T-1} \mathbb{E}_{v_{[T-1]}} [V(x_k, u_k, d)] \\
&\stackrel{(s.2)}{\leq} \frac{\mu}{2\alpha_2 T} \cdot \sqrt{\frac{c_{21}}{c_{12}}} \cdot \left[\left(\rho^{T-1} + \frac{1}{1-\rho} \right) B_0 \right. \\
&\quad \left. + \frac{T-1}{1-\rho} \left(d_1 + \sqrt{\frac{c_{12}}{c_{21}}} d_2 \right) \right], \quad (52)
\end{aligned}$$

where (s.1) follows from (32) in Appendix A and the definition (5) of μ , and (s.2) uses (48) in Appendix F. Based on the mentioned parametric conditions and the orders of terms obtained in Appendix F, the bound in (52) is of the order of

$$\mathcal{O}\left(\frac{\epsilon^{\frac{3}{2}} \sqrt{\mu}}{\sqrt{pT}(1-\rho)}\right) + \mathcal{O}\left(\frac{(\epsilon^2 + \frac{1}{T\alpha_2})\mu}{1-\rho}\right).$$

I. Proof of Theorem 8

Based on Lemma 7, $\tilde{\Phi}_\delta(w)$ is $L(=Mp/\delta)$ -smooth. Hence,

$$\begin{aligned}
&\tilde{\Phi}_\delta(w_{k+1}) \\
&\leq \tilde{\Phi}_\delta(w_k) + \nabla \tilde{\Phi}_\delta^\top(w_k)(w_{k+1} - w_k) + \frac{L}{2} \|w_{k+1} - w_k\|^2 \\
&= \tilde{\Phi}_\delta(w_k) + \eta \nabla \tilde{\Phi}_\delta^\top(w_k)(s_k - w_k) + \frac{L\eta^2}{2} \|s_k - w_k\|^2, \quad (53)
\end{aligned}$$

where the equality follows from the update (24). Let

$$\hat{s}_k = \arg \min_{s \in \mathcal{U}} \langle s, \nabla \tilde{\Phi}_\delta(w_k) \rangle$$

be an auxiliary variable. It follows from the calculation of s_k (24b) and the definition of $\mathcal{G}(w_k)$ (25) that

$$\langle s_k, \tilde{\phi}_k \rangle \leq \langle \hat{s}_k, \tilde{\phi}_k \rangle, \quad (54a)$$

$$\begin{aligned}
-\mathcal{G}(w_k) &= \min_{s \in \mathcal{U}} \langle s - w_k, \nabla \tilde{\Phi}_\delta(w_k) \rangle \\
&= \langle \hat{s}_k - w_k, \nabla \tilde{\Phi}_\delta(w_k) \rangle. \quad (54b)
\end{aligned}$$

For the middle term of the upper bound in (53), we have

$$\begin{aligned}
&\eta \nabla \tilde{\Phi}_\delta^\top(w_k)(s_k - w_k) \\
&\stackrel{(s.1)}{=} \eta \tilde{\phi}_k^\top(s_k - w_k) + \eta (\nabla \tilde{\Phi}_\delta(w_k) - \tilde{\phi}_k)^\top(s_k - w_k) \\
&\stackrel{(s.2)}{\leq} \eta \tilde{\phi}_k^\top(\hat{s}_k - w_k) + \eta (\nabla \tilde{\Phi}_\delta(w_k) - \tilde{\phi}_k)^\top(s_k - w_k) \\
&\stackrel{(s.3)}{=} \eta \nabla \tilde{\Phi}_\delta^\top(w_k)(\hat{s}_k - w_k) + \eta (\tilde{\phi}_k - \nabla \tilde{\Phi}_\delta(w_k))^\top(s_k - \hat{s}_k) \\
&\stackrel{(s.4)}{=} -\eta \mathcal{G}(w_k) + \eta \|\tilde{\phi}_k - \nabla \tilde{\Phi}_\delta(w_k)\| \|s_k - \hat{s}_k\|, \quad (55)
\end{aligned}$$

where (s.1) is obtained by adding and subtracting $\eta \tilde{\phi}_k^\top(s_k - w_k)$; (s.2) follows from (54a); (s.3) follows by adding and subtracting $\nabla \tilde{\Phi}_\delta^\top(w_k)(\hat{s}_k - w_k)$; (s.4) uses (54b) and the Cauchy-Schwarz inequality. We incorporate (55) into (53), take expectations of both sides of the inequality with respect to $v_{[k]}$, and obtain

$$\begin{aligned}
&\mathbb{E}_{v_{[k]}} [\tilde{\Phi}_\delta(w_{k+1})] \\
&\leq \mathbb{E}_{v_{[k]}} [\tilde{\Phi}_\delta(w_k)] - \eta \mathbb{E}_{v_{[k]}} [\mathcal{G}(w_k)] + \frac{L\eta^2}{2} \mathbb{E}_{v_{[k]}} [\|s_k - w_k\|^2] \\
&\quad + \eta \mathbb{E}_{v_{[k]}} [\|\tilde{\phi}_k - \nabla \tilde{\Phi}_\delta(w_k)\| \|s_k - \hat{s}_k\|] \\
&\leq \mathbb{E}_{v_{[k]}} [\tilde{\Phi}_\delta(w_k)] - \eta \mathbb{E}_{v_{[k]}} [\mathcal{G}(w_k)] + \frac{L\eta^2 D^2}{2}
\end{aligned}$$

$$+ \eta D \mathbb{E}_{v_{[k]}} [\|\tilde{\phi}_k - \nabla \tilde{\Phi}_\delta(w_k)\|],$$

where the last inequality holds since \mathcal{U} is bounded with diameter D , and the update (24a) and the choice of η guarantee that $s_k, \hat{s}_k, w_k \in \mathcal{U}$. By rearranging terms, telescoping sums and dividing both sides of the inequality by T , we have

$$\begin{aligned}
&\frac{1}{T} \sum_{k=1}^T \mathbb{E}_{v_{[T]}} [\mathcal{G}(w_k)] \\
&\leq \frac{1}{\eta T} (\mathbb{E}_{v_{[T]}} [\tilde{\Phi}_\delta(w_1)] - \mathbb{E}_{v_{[T]}} [\tilde{\Phi}_\delta(w_{T+1})]) + \frac{L\eta D^2}{2} \\
&\quad + \frac{D}{T} \sum_{k=1}^T \mathbb{E}_{v_{[T]}} [\|\tilde{\phi}_k - \nabla \tilde{\Phi}_\delta(w_k)\|]. \quad (56)
\end{aligned}$$

We now provide a bound for the last term of (56). Based on the AM-QM inequality, we have

$$\begin{aligned}
&\frac{1}{T} \sum_{k=1}^T \mathbb{E}_{v_{[T]}} [\|\tilde{\phi}_k - \nabla \tilde{\Phi}_\delta(w_k)\|] \\
&\leq \sqrt{\frac{1}{T} \sum_{k=1}^T \mathbb{E}_{v_{[T]}} [\|\tilde{\phi}_k - \nabla \tilde{\Phi}_\delta(w_k)\|^2]}. \quad (57)
\end{aligned}$$

Next, we focus on the bound for the second moment $\mathbb{E}[\|\tilde{\phi}_k - \nabla \tilde{\Phi}_\delta(w_k)\|^2]$. Note that

$$\begin{aligned}
&\mathbb{E}_{v_{[k]}} [\|\tilde{\phi}_k - \nabla \tilde{\Phi}_\delta(w_k)\|^2] \\
&= \frac{p^2}{\delta^2} \mathbb{E}_{v_{[k]}} [\|v_k(\Phi(u_k, y_{k+1}) - \Phi(u_{k-1}, y_k)) - \nabla \tilde{\Phi}_\delta(w_k)\|^2] \\
&= \frac{p^2}{\delta^2} \mathbb{E}_{v_{[k]}} [\|v_k(\tilde{\Phi}(u_k) - \tilde{\Phi}(u_{k-1})) - \nabla \tilde{\Phi}_\delta(w_k) \\
&\quad + v_k(e_\Phi(x_k, u_k) - e_\Phi(x_{k-1}, u_{k-1}))\|^2] \\
&\stackrel{(s.1)}{\leq} \underbrace{\frac{3p^2}{\delta^2} \mathbb{E}_{v_{[k]}} [\|v_k(\tilde{\Phi}(u_k) - \tilde{\Phi}(u_{k-1})) - \nabla \tilde{\Phi}_\delta(w_k)\|^2]}_{\textcircled{1}} \\
&\quad + \underbrace{\frac{3p^2}{\delta^2} (\mathbb{E}_{v_{[k]}} [\|v_k e_\Phi(x_k, u_k)\|^2] + \mathbb{E}_{v_{[k]}} [\|v_k e_\Phi(x_{k-1}, u_{k-1})\|^2])}_{\textcircled{2}}, \quad (58)
\end{aligned}$$

where (s.1) follows from the AM-QM inequality. Then, we provide bounds on the two terms of (58) in order.

For term $\textcircled{1}$ in (58),

$$\begin{aligned}
\textcircled{1} &\stackrel{(s.1)}{\leq} \frac{3p^2}{\delta^2} \mathbb{E}_{v_{[k]}} [\|v_k(\tilde{\Phi}(u_k) - \tilde{\Phi}(u_{k-1}))\|^2] \\
&= \frac{3p^2}{\delta^2} \mathbb{E}_{v_{[k]}} [\|v_k(\tilde{\Phi}(w_k + \delta v_k) - \tilde{\Phi}(w_{k-1} + \delta v_k) \\
&\quad + \tilde{\Phi}(w_{k-1} + \delta v_k) - \tilde{\Phi}(w_{k-1} + \delta v_{k-1}))\|^2] \\
&\stackrel{(s.2)}{\leq} \frac{6p^2}{\delta^2} \mathbb{E}_{v_{[k]}} [\|v_k(\tilde{\Phi}(w_k + \delta v_k) - \tilde{\Phi}(w_{k-1} + \delta v_k))\|^2 \\
&\quad + \|v_k(\tilde{\Phi}(w_{k-1} + \delta v_k) - \tilde{\Phi}(w_{k-1} + \delta v_{k-1}))\|^2] \\
&\stackrel{(s.3)}{\leq} \frac{6M^2 p^2}{\delta^2} \mathbb{E}_{v_{[k]}} [\|w_k - w_{k-1}\|^2 \|v_k\|^2 \\
&\quad + \delta^2 \|v_k - v_{k-1}\|^2 \|v_k\|^2] \\
&\stackrel{(s.4)}{\leq} \frac{6M^2 p^2}{\delta^2} (\mathbb{E}_{v_{[k]}} [\eta^2 \|s_{k-1} - w_{k-1}\|^2]
\end{aligned}$$

$$\begin{aligned}
& + \delta^2 \mathbb{E}_{v_{[k]}} [2(\|v_k\|^2 + \|v_{k-1}\|^2)\|v_k\|^2]) \\
& \stackrel{(s.5)}{\leq} \frac{6M^2 p^2}{\delta^2} (\eta^2 D^2 + 4\delta^2).
\end{aligned}$$

In (s.1), we utilize the property that the variance is not more than the second moment, given that

$$\begin{aligned}
& \mathbb{E}_{v_{[k]}} [v_k(\tilde{\Phi}(u_k) - \tilde{\Phi}(u_{k-1}))] \\
& = \mathbb{E}_{v_{[k]}} [v_k(\tilde{\Phi}(w_k + \delta v_k) - \tilde{\Phi}(w_{k-1} + \delta v_{k-1}))] \\
& \stackrel{(e.1)}{=} \mathbb{E}_{v_{[k]}} [v_k \tilde{\Phi}(w_k + \delta v_k)] \\
& \stackrel{(e.2)}{=} \nabla \tilde{\Phi}_\delta(w_k),
\end{aligned}$$

where (e.1) follows from the independence of $\tilde{\Phi}(w_{k-1} + \delta v_{k-1})$ on v_k and $\mathbb{E}_{v_{[k]}}[v_k] = 0$, and (e.2) uses (23a). Furthermore, (s.2) relies on the inequality $\mathbb{E}[(a+b)^2] \leq 2\mathbb{E}[a^2 + b^2]$, $\forall a, b$; (s.3) uses the assumption that $\tilde{\Phi}(u)$ is M -Lipschitz; (s.4) follows from the update (24a) and the inequality $\|a-b\|^2 \leq 2(\|a\|^2 + \|b\|^2)$, $\forall a, b$; (s.5) holds because $s_{k-1}, w_{k-1} \in \mathcal{U}$ and \mathcal{U} is bounded with diameter D .

Then, we bound term ② in (58).

$$\begin{aligned}
\textcircled{2} & \stackrel{(s.1)}{=} \frac{3p^2}{\delta^2} (\mathbb{E}_{v_{[k]}} [|e_\Phi(x_k, u_k)|^2] + \mathbb{E}_{v_{[k]}} [|e_\Phi(x_{k-1}, u_{k-1})|^2]) \\
& \stackrel{(s.2)}{\leq} \frac{3p^2 M_y^2 M_g^2}{\alpha_1 \delta^2} \left(1 - \frac{\alpha_3}{\alpha_2}\right) \\
& \quad \cdot (\mathbb{E}_{v_{[k]}} [V(x_k, u_k, d)] + \mathbb{E}_{v_{[k]}} [V(x_{k-1}, u_{k-1}, d)]),
\end{aligned}$$

where (s.1) uses the fact that $\|v_k\| = 1$, since $v_k \sim U(\mathbb{S}_{p-1})$; (s.2) follows from the bound on $|e_\Phi(x_k, u_k)|^2$ in (11).

Next, we focus on the recursive inequality of the expected value of the Lyapunov function, i.e., $\mathbb{E}_{v_{[k]}} [V(x_k, u_k, d)]$. The inequality (33) in Appendix B still holds. Note that we use the new update rule (24) and draw v_k, v_{k-1} from the unit sphere. Hence, the bound on $\mathbb{E}_{v_{[k]}} [\|u_k - u_{k-1}\|^2]$ is given by

$$\begin{aligned}
\mathbb{E}_{v_{[k]}} [\|u_k - u_{k-1}\|^2] & = \mathbb{E}_{v_{[k]}} [\|w_k - w_{k-1} + \delta v_k - \delta v_{k-1}\|^2] \\
& \stackrel{(s.1)}{\leq} \mathbb{E}_{v_{[k]}} [2\|w_k - w_{k-1}\|^2 + 2\delta^2 \|v_k - v_{k-1}\|^2] \\
& \stackrel{(s.2)}{\leq} \mathbb{E}_{v_{[k]}} [2\eta^2 \|s_{k-1} - w_{k-1}\|^2 + 4\delta^2 (\|v_k\|^2 + \|v_{k-1}\|^2)] \\
& \stackrel{(s.3)}{\leq} 2\eta^2 D^2 + 8\delta^2,
\end{aligned}$$

where (s.1) uses the inequality $\mathbb{E}[(a+b)^2] \leq 2\mathbb{E}[a^2 + b^2]$, $\forall a, b$; (s.2) follows from the update (24a) and the inequality $\|a-b\|^2 \leq 2(\|a\|^2 + \|b\|^2)$, $\forall a, b$; (s.3) relies on the fact that s_{k-1} and w_{k-1} lie in the bounded set \mathcal{U} with diameter D , and that $\|v_k\| = 1$. Therefore,

$$\begin{aligned}
\mathbb{E}_{v_{[k]}} [V(x_k, u_k, d)] & \leq \frac{2\alpha_2}{\alpha_1} \left(1 - \frac{\alpha_3}{\alpha_2}\right) \mathbb{E}_{v_{[k]}} [V(x_{k-1}, u_{k-1}, d)] \\
& \quad + 2\alpha_2 M_x^2 (2\eta^2 D^2 + 8\delta^2). \quad (59)
\end{aligned}$$

It follows that

$$\begin{aligned}
& \frac{1}{T} \sum_{k=0}^{T-1} \mathbb{E}_{v_{[T]}} [V(x_k, u_k, d)] \\
& \leq \frac{\mathbb{E}_{v_{[T]}} [V(x_0, u_0, d)] + 2(T-1)\alpha_2 M_x^2 (2\eta^2 D^2 + 8\delta^2)}{\left[1 - \frac{2\alpha_2}{\alpha_1} \left(1 - \frac{\alpha_3}{\alpha_2}\right)\right] T}.
\end{aligned}$$

By incorporating the obtained bounds on terms ① and ② as well as (59) into (58), we have

$$\begin{aligned}
& \frac{1}{T} \sum_{k=1}^T \mathbb{E}_{v_{[T]}} [\|\tilde{\phi}_k - \nabla \tilde{\Phi}_\delta(w_k)\|^2] \leq \\
& \frac{3p^2}{\delta^2} \left(2M^2 (\eta^2 D^2 + 4\delta^2) + \frac{M_y^2 M_g^2}{\alpha_1} \left(1 - \frac{\alpha_3}{\alpha_2}\right) \right. \\
& \quad \cdot \left(\left[1 + \frac{2\alpha_2}{\alpha_1} \left(1 - \frac{\alpha_3}{\alpha_2}\right)\right] \frac{1}{T} \sum_{k=0}^{T-1} \mathbb{E}_{v_{[T]}} [V(x_k, u_k, d)] \right. \\
& \quad \left. \left. + 2\alpha_2 M_x^2 (2\eta^2 D^2 + 8\delta^2) \right) \right). \quad (60)
\end{aligned}$$

To guarantee that $\|\tilde{\Phi}_\delta(u) - \tilde{\Phi}(u)\| \leq \epsilon$, we set $\delta = \frac{\epsilon}{M}$. We combine (56), (57) and (60) and obtain

$$\begin{aligned}
& \frac{1}{T} \sum_{k=1}^T \mathbb{E}_{v_{[T]}} [\mathcal{G}(w_k)] \leq \\
& \frac{\mathbb{E}_{v_{[T]}} [\tilde{\Phi}_\delta(w_1)] - \tilde{\Phi}_\delta^*}{\eta T} + \frac{D^2 M p}{2} \cdot \frac{\eta}{\delta} + D \left\{ \right. \\
& 6M^2 D^2 p^2 \frac{\eta^2}{\delta^2} + 24M^2 p^2 + \frac{M_y^2 M_g^2}{\alpha_1} \left(1 - \frac{\alpha_3}{\alpha_2}\right) \\
& \quad \cdot \left[\frac{1 + \frac{2\alpha_2}{\alpha_1} \left(1 - \frac{\alpha_3}{\alpha_2}\right)}{\left[1 - \frac{2\alpha_2}{\alpha_1} \left(1 - \frac{\alpha_3}{\alpha_2}\right)\right] T} \cdot \left(\mathbb{E}_{v_{[T]}} [V(x_0, u_0, d)] \right. \right. \\
& \quad \left. \left. + 2(T-1)\alpha_2 M_x^2 (2D^2 \eta^2 + 8\delta^2) \right) \right. \\
& \quad \left. \left. + 2\alpha_2 M_x^2 (2D^2 \eta^2 + 8\delta^2) \right] \right\}^{\frac{1}{2}}, \quad (61)
\end{aligned}$$

where we use the fact that $\mathbb{E}[\tilde{\Phi}_\delta(w_{T+1})] \geq \tilde{\Phi}_\delta^* \triangleq \inf_{u \in \mathcal{U}} \tilde{\Phi}_\delta(u)$. Note that $\tilde{\Phi}_\delta^*$ is finite, since $\inf_{u \in \mathcal{U}} \tilde{\Phi}(u)$ is finite (see (20)) and $\tilde{\Phi}_\delta(u)$ is close to $\tilde{\Phi}(u)$ (see Lemma 7). Then, we set $\eta = \kappa \sqrt{\frac{\epsilon}{pT}}$ such that $\frac{1}{\eta T}$ and $\frac{p\eta}{\delta}$ are of the same order. Also, κ falls in $(0, \frac{\sqrt{pT}}{\sqrt{\epsilon}})$ to ensure that $\eta \in (0, 1)$. Consequently, for any $k \in \mathbb{N}$, w_{k+1} is a convex combination of w_k and s_k and lies in \mathcal{U} provided that $w_0 \in \mathcal{U}$. By plugging the expressions of δ and η into (61) and using the definition (5) of μ , we arrive at (26).

ACKNOWLEDGMENT

The authors would like to thank Dr. Giuseppe Belgioioso, Dr. Dominic Liao-McPherson, Lukas Ortmann, Keith Moffat, Miguel Picallo, and Jialun Li for enlightening discussions.

REFERENCES

- [1] Y. Nesterov, *Lectures on convex optimization*. Berlin, Germany: Springer, 2018, vol. 137.
- [2] K. B. Ariyur and M. Krstic, *Real-time optimization by extremum-seeking control*. Hoboken, NJ, USA: John Wiley & Sons, 2003.
- [3] C. Manzie and M. Krstic, "Extremum seeking with stochastic perturbations," *IEEE Transactions on Automatic Control*, vol. 54, no. 3, pp. 580–585, 2009.
- [4] S.-J. Liu and M. Krstic, "Stochastic averaging in discrete time and its applications to extremum seeking," *IEEE Transactions on Automatic Control*, vol. 61, no. 1, pp. 90–102, 2016.
- [5] A. Ghaffari, M. Krstić, and D. Nešić, "Multivariable Newton-based extremum seeking," *Automatica*, vol. 48, no. 8, pp. 1759–1767, 2012.
- [6] S.-J. Liu and M. Krstic, "Newton-based stochastic extremum seeking," *Automatica*, vol. 50, no. 3, pp. 952–961, 2014.

- [7] J. C. Spall, "Multivariate stochastic approximation using a simultaneous perturbation gradient approximation," *IEEE Transactions on Automatic Control*, vol. 37, no. 3, pp. 332–341, 1992.
- [8] M. Guay, E. Moshksar, and D. Dochain, "A constrained extremum-seeking control approach," *International Journal of Robust and Non-linear Control*, vol. 25, no. 16, pp. 3132–3153, 2015.
- [9] R. S. Sutton and A. G. Barto, *Reinforcement learning: An introduction*. Cambridge, MA, USA: MIT Press, 2018.
- [10] A. Hauswirth, S. Bolognani, G. Hug, and F. Dörfler, "Optimization algorithms as robust feedback controllers," *arXiv preprint arXiv:2103.11329*, 2021.
- [11] A. Simonetto, E. Dall'Anese, S. Paternain, G. Leus, and G. B. Giannakis, "Time-varying convex optimization: Time-structured algorithms and applications," *Proceedings of the IEEE*, vol. 108, no. 11, pp. 2032–2048, 2020.
- [12] A. Marchetti, B. Chachuat, and D. Bonvin, "Modifier-adaptation methodology for real-time optimization," *Industrial & Engineering Chemistry Research*, vol. 48, no. 13, pp. 6022–6033, 2009.
- [13] M. Diehl, H. G. Bock, and J. P. Schlöder, "A real-time iteration scheme for nonlinear optimization in optimal feedback control," *SIAM Journal on Control and Optimization*, vol. 43, no. 5, pp. 1714–1736, 2005.
- [14] M. N. Zeilinger, C. N. Jones, and M. Morari, "Real-time suboptimal model predictive control using a combination of explicit MPC and online optimization," *IEEE Transactions on Automatic Control*, vol. 56, no. 7, pp. 1524–1534, 2011.
- [15] E. Dall'Anese and A. Simonetto, "Optimal power flow pursuit," *IEEE Transactions on Smart Grid*, vol. 9, no. 2, pp. 942–952, 2016.
- [16] Y. Tang, K. Dvijotham, and S. Low, "Real-time optimal power flow," *IEEE Transactions on Smart Grid*, vol. 8, no. 6, pp. 2963–2973, 2017.
- [17] S. H. Low, F. Paganini, and J. C. Doyle, "Internet congestion control," *IEEE Control Systems Magazine*, vol. 22, no. 1, pp. 28–43, 2002.
- [18] M. Colombino, J. W. Simpson-Porco, and A. Bernstein, "Towards robustness guarantees for feedback-based optimization," in *Proc. 58th IEEE Conference on Decision and Control*, 2019, pp. 6207–6214.
- [19] L. Ortmann, A. Hauswirth, I. Caduff, F. Dörfler, and S. Bolognani, "Experimental validation of feedback optimization in power distribution grids," *Electric Power Systems Research*, vol. 189, p. 106782, 2020.
- [20] A. Bernstein, E. Dall'Anese, and A. Simonetto, "Online primal-dual methods with measurement feedback for time-varying convex optimization," *IEEE Transactions on Signal Processing*, vol. 67, no. 8, pp. 1978–1991, 2019.
- [21] M. Colombino, E. Dall'Anese, and A. Bernstein, "Online optimization as a feedback controller: Stability and tracking," *IEEE Transactions on Control of Network Systems*, vol. 7, no. 1, pp. 422–432, 2020.
- [22] Y. Tang, E. Dall'Anese, A. Bernstein, and S. H. Low, "A feedback-based regularized primal-dual gradient method for time-varying nonconvex optimization," in *Proc. 57th IEEE Conference on Decision and Control*, 2018, pp. 3244–3250.
- [23] Y. Chen, A. Bernstein, A. Devraj, and S. Meyn, "Model-free primal-dual methods for network optimization with application to real-time optimal power flow," in *Proc. American Control Conference*, 2020, pp. 3140–3147.
- [24] M. Nonhoff and M. A. Müller, "Online gradient descent for linear dynamical systems," *Proc. IFAC World Congress*, pp. 945–952, 2020.
- [25] E. Dall'Anese, A. Simonetto, S. Becker, and L. Madden, "Optimization and learning with information streams: Time-varying algorithms and applications," *IEEE Signal Processing Magazine*, vol. 37, no. 3, pp. 71–83, 2020.
- [26] V. Häberle, A. Hauswirth, L. Ortmann, S. Bolognani, and F. Dörfler, "Non-convex feedback optimization with input and output constraints," *IEEE Control Systems Letters*, vol. 5, no. 1, pp. 343–348, 2020.
- [27] S. Menta, A. Hauswirth, S. Bolognani, G. Hug, and F. Dörfler, "Stability of dynamic feedback optimization with applications to power systems," in *Proc. 56th Annual Allerton Conference on Communication, Control, and Computing*, 2018, pp. 136–143.
- [28] A. Hauswirth, S. Bolognani, G. Hug, and F. Dörfler, "Timescale separation in autonomous optimization," *IEEE Transactions on Automatic Control*, vol. 66, no. 2, pp. 611–624, 2020.
- [29] G. Bianchin, M. Vaquero, J. Cortés, and E. Dall'Anese, "Online stochastic optimization for unknown linear systems: Data-driven synthesis and controller analysis," *arXiv preprint arXiv:2108.13040*, 2021.
- [30] G. Belgioioso, D. Liao-McPherson, M. H. de Badyn, S. Bolognani, J. Lygeros, and F. Dörfler, "Sampled-data online feedback equilibrium seeking: Stability and tracking," in *Proc. 60th IEEE Conference on Decision and Control*, 2021, pp. 2702–2708.
- [31] A. Hauswirth, S. Bolognani, and F. Dörfler, "Projected dynamical systems on irregular, non-euclidean domains for nonlinear optimization," *SIAM Journal on Control and Optimization*, vol. 59, no. 1, pp. 635–668, 2021.
- [32] M. Picallo, L. Ortmann, S. Bolognani, and F. Dörfler, "Adaptive real-time grid operation via online feedback optimization with sensitivity estimation," *arXiv preprint arXiv:2110.00954*, 2021.
- [33] M. Nonhoff and M. A. Müller, "Data-driven online convex optimization for control of dynamical systems," in *Proc. 60th IEEE Conference on Decision and Control*, 2021, pp. 3640–3645.
- [34] D. K. Molzahn, F. Dörfler, H. Sandberg, S. H. Low, S. Chakrabarti, R. Baldick, and J. Lavaei, "A survey of distributed optimization and control algorithms for electric power systems," *IEEE Transactions on Smart Grid*, vol. 8, no. 6, pp. 2941–2962, 2017.
- [35] R. S. Sutton, D. A. McAllester, S. P. Singh, Y. Mansour *et al.*, "Policy gradient methods for reinforcement learning with function approximation," in *Proc. NIPS*, vol. 99, 1999, pp. 1057–1063.
- [36] D. Silver, G. Lever, N. Heess, T. Degris, D. Wierstra, and M. Riedmiller, "Deterministic policy gradient algorithms," in *Proc. ICML*, 2014, pp. 387–395.
- [37] S. Liu, P.-Y. Chen, B. Kailkhura, G. Zhang, A. O. Hero III, and P. K. Varshney, "A primer on zeroth-order optimization in signal processing and machine learning: Principals, recent advances, and applications," *IEEE Signal Processing Magazine*, vol. 37, no. 5, pp. 43–54, 2020.
- [38] Y. Nesterov and V. Spokoiny, "Random gradient-free minimization of convex functions," *Foundations of Computational Mathematics*, vol. 17, no. 2, pp. 527–566, 2017.
- [39] J. C. Duchi, M. I. Jordan, M. J. Wainwright, and A. Wibisono, "Optimal rates for zero-order convex optimization: The power of two function evaluations," *IEEE Transactions on Information Theory*, vol. 61, no. 5, pp. 2788–2806, 2015.
- [40] O. Shamir, "An optimal algorithm for bandit and zero-order convex optimization with two-point feedback," *Journal of Machine Learning Research*, vol. 18, no. 1, pp. 1703–1713, 2017.
- [41] A. D. Flaxman, A. T. Kalai, and H. B. McMahan, "Online convex optimization in the bandit setting: gradient descent without a gradient," in *Proc. 16th Annual ACM-SIAM Symposium on Discrete Algorithms*, 2005, pp. 385–394.
- [42] Y. Zhang, Y. Zhou, K. Ji, and M. M. Zavlanos, "Improving the convergence rate of one-point zeroth-order optimization using residual feedback," *arXiv preprint arXiv:2006.10820*, 2020.
- [43] A. L. Dontchev and R. T. Rockafellar, *Implicit functions and solution mappings*. New York, NY, USA: Springer, 2009, vol. 543.
- [44] H. Khalil, *Nonlinear Systems*. Upper Saddle River, NJ, USA: Prentice Hall, 2002.
- [45] N. Bof, R. Carli, and L. Schenato, "Lyapunov theory for discrete time systems," *arXiv preprint arXiv:1809.05289*, 2018.
- [46] S. Ghadimi and G. Lan, "Stochastic first-and zeroth-order methods for nonconvex stochastic programming," *SIAM Journal on Optimization*, vol. 23, no. 4, pp. 2341–2368, 2013.
- [47] X. Gao, B. Jiang, and S. Zhang, "On the information-adaptive variants of the ADMM: an iteration complexity perspective," *Journal of Scientific Computing*, vol. 76, no. 1, pp. 327–363, 2018.
- [48] J. Chen, D. Zhou, J. Yi, and Q. Gu, "A Frank-Wolfe framework for efficient and effective adversarial attacks," in *Proc. AAAI*, vol. 34, no. 04, 2020, pp. 3486–3494.
- [49] M. Jaggi, "Revisiting Frank-Wolfe: Projection-free sparse convex optimization," in *Proc. ICML*, 2013, pp. 427–435.
- [50] K. Balasubramanian and S. Ghadimi, "Zeroth-order nonconvex stochastic optimization: Handling constraints, high dimensionality, and saddle points," *Foundations of Computational Mathematics*, pp. 1–42, 2021.
- [51] A. K. Sahu, M. Zaheer, and S. Kar, "Towards gradient free and projection free stochastic optimization," in *Proc. AISTATS*, 2019, pp. 3468–3477.
- [52] S. Boyd and L. Vandenberghe, *Convex optimization*. Cambridge, U.K.: Cambridge University Press, 2004.
- [53] M. R. Metel and A. Takeda, "Stochastic proximal methods for non-smooth non-convex constrained sparse optimization," *Journal of Machine Learning Research*, vol. 22, no. 115, pp. 1–36, 2021.
- [54] R. A. Horn and C. R. Johnson, *Matrix analysis*. Cambridge, U.K.: Cambridge University Press, 2012.